Electronic Supplementary Material (ESI) for Chemical Science.

(Supporting Information)

Hierarchical Covalent Organic Framework-foam for Multi-enzyme Tandem Catalysis

Satyadip Paul,[ab] Mani Gupta,[c] Kaushik Dey,[ab] Ashok Kumar Mahato,[ab] Saikat Bag,[ab] Arun Torris,[d] E. Bhoje Gowd,[e] Hasnain Sajid,[f] Matthew A. Addicoat,[f] Supratim Datta[c]* and Rahul Banerjee[ab]*

[a]Department of Chemical Sciences, Indian Institute of Science Education and Research, Kolkata, Mohanpur 741246, India.

[b]Centre for Advanced Functional Materials, Indian Institute of Science Education and Research, Kolkata, Mohanpur 741246, India.

[c]Department of Biological Sciences, and Center for the Climate and Environmental Sciences, Indian Institute of Science Education and Research Kolkata, Mohanpur 741246, India.

[d]Polymer Science and Engineering Division, CSIR-National Chemical Laboratory, Dr. Homi Bhabha Road, Pune 411008, India

[e]Materials Science and Technology Division, CSIR-National Institute for Interdisciplinary Science and Technology, Trivandrum 695 019, Kerala, India.

[f]School of Science and Technology, Nottingham Trent University, NG11 8NS Nottingham.

*Email: supratim@iiserkol.ac.in; Tel: +033-6136-0000-1219.

*Email: r.banerjee@iiserkol.ac.in; Tel: +033-6136-0000-1327.

Table of Contents

Section S-1: Materials and Instrumentation

Materials

The starting material 1,3,5–triformylphloroglucinol (Tp), was synthesized by the previously reported protocols[1-2]. All commercially available reagents and solvents were used without further purification. All the commercially available materials such as 4,4'-azodianiline (Azo), Potassium hydrogen phosphate, potassium dihydrogen phosphate, sodium bicarbonate, sodium carboxymethylcellulose (CMC), *p*-nitrophenyl-β-D-glucopyranoside (*p*NPGlc), 3,5-dinitrosalicylic acid (DNS), saturated phenol, HEPES free acid, glycine, citric acid, bovine serum albumin (BSA) and solvents were bought from Sigma-Aldrich, TCI chemicals, Avra chemicals, and Fisher Scientific, SRL chemicals, MP biomedicals depending upon their availability. Protein molecular weight marker was purchased from Thermofisher Scientific, Mumbai, India. The pBAD bacterial expression plasmid was obtained from Thermo Fisher Scientific, Waltham, USA. *Escherichia coli* Top 10F′ cells were purchased from Life Technologies, La Jolla, CA, USA. A total of 30 kDa cutoff size Amicon-Ultra-15 membranes were obtained from EMD Millipore, Billerica, USA. Coomassie brilliant blue from Sigma Aldrich USA. All the catalysis reactions were performed under open air in the respective buffer as the reaction medium in heterogeneous conditions.

General instrumentations and methods

Powder X-ray diffraction (PXRD) data were collected using a XEUSS system using a Genix micro source from Xenocs operated at 50 kV and 0.6 mA. The Cu K_α radiation (λ = 1.54 Å) was collimated with FOX2D mirror and two pairs of less scattering slits from Xenocs. The 2D patterns were recorded on a Mar345 image plate and processed using Fit2D software. All the measurements have been made in the transmission mode. The sample to detector distance calibrated with silver behenate standard is 220.8 mm for PXRD measurement. To calculate the unit cell parameters, two possible stacking models (eclipsed AA and staggered AB) were built using Accelrys, Material Studio-6 software using the Self-Consistent Charge Density Functional Tight-Binding (SCC-DFTB) method (*J. Am. Chem. Soc*. **2012**, *134*, 19524; *J. Am. Chem. Soc*. **2013**, *135*, 17853). Several stacking possibilities are considered for reasons reported in the literature.

Fourier transform infrared (FTIR) spectra have been collected using a Bruker Optics ALPHAE spectrometer with a universal Zn-Se ATR (attenuated total reflection) accessory. FTIR data are reported with a wavenumber (cm^{-1}) scale.

Scanning Electron Microscopy (SEM) measurements have been executed with a Zeiss SUPRA 55 VP scanning electron microscope and Zeiss SIGMA Scanning Electron Microscope equipped with tungsten filament as electron source operated at 10 kV. The samples are prepared simply by putting a drop of COFs dispersed in isopropanol or dichloromethane on a clean piece of Silicon wafer. To avoid charging during SEM analyses, we coated all the COFs samples with a thin layer of gold with an SCD 040 Balzers Union before analyses.

Transmission Electron Microscopy (TEM) analyses have been performed using a UHR-FEGTEM, DST-FIST facility of IISER Kolkata at an accelerating voltage of 200 kV. The TEM samples were prepared for analysis by drop-casting the samples (dispersed in isopropanol) on copper grids TEM Window (TED PELLA, INC. 200 mesh).

N_2 adsorption analyses have been performed at 77 K using a liquid nitrogen bath (77 K) on a Quantachrome Quadrasorb automatic volumetric instrument. All COFs samples were outgassed for 12 h at 120 °C under vacuum before the gas adsorption studies. The surface areas were evaluated using the Brunauer-Emmett-Teller (BET) model applied between P/P_0 values of 0.05 and 0.3 for mesoporous COFs. The pore size distributions were calculated using the non-localized density functional theory (NLDFT) method. Each COF's surface area was measured multiple times and then averaged out for proper comparison.

Ultraviolet-Visible Spectroscopy (UV-vis) data were measured using UV-visible absorption spectra measured using Agilent 8453 UV-vis spectrophotometer at room temperature.

Confocal Laser Scanning Microscopy (CLSM) images were collected using Carl Zeiss LSM 710 confocal workstation. The instrument has EC Epiplan-APOCHROMAT objective of 50X magnification and a numerical aperture of 0.9. Fluorescence from the sample was excited with the 488-nm line of an Argon laser. The fluorescence was separated from the excitation light by band-pass sliders (493 nm-619 nm) in front of spectral detectors. The microscope objective has been attached to an opto-electronically coded focus z-driver to scan the objective along the vertical z direction and produce three-dimensional images. A pinhole was used to reject the out-of-plane light for background rejection hence a better signal-to-noise ratio. We typically acquired 150–200 sliced stacks of 512 X 512 pixel images in the horizontal x–y plain separated by 0.25 μm in the z-direction. The length of the full-sized field of view is approximately 283 μm and a depth of approximately 40 μm. The images were processed using the Zen software (Zeiss, Oberkochen).

Plate reader: Plate reader of SpectraMax M2 from Molecular Device was used for the absorbance measurements for the assays at room temperature.

SDS-PAGE: SDS-PAGE was done according to the standard Laemmli (1970) procedure in 10 % polyacrylamide gels. PageRuler™ Plus Prestained SDS-PAGE (Thermofisher, Mumbai, India) was used as the molecular weight marker. For protein visualization, gels were stained with Coomassie brilliant blue.

3D X-ray Tomography Imaging of Foams was imaged using X-ray microtomography (Xradia 510 Versa X-ray Microscope, Zeiss X-ray Microscopy, Pleasanton, CA, USA) to study the morphology and characteristics of pores in it. Foams were loaded onto the sample holder and kept between the X-ray source and the detector assembly. Detector assembly consisted of a scintillator, 20 X optics, and a CCD camera. The X-ray source was ramped up to 60 kV and 5 W. The tomographic image acquisitions were completed by acquiring 3201 projections over 360° of rotation with a pixel size of approximately 0.8 microns for a field of view of approximately 1 x 1 x 1 mm^3. Each projection was recorded with 8 seconds of exposure time. In addition, projections without the specimen in the beam (reference images) were also collected and averaged. The filtered back-projection algorithm was used for the reconstruction of the projections to generate two-dimensional (2D) virtual cross-sections of the specimens.

Segmentation and further processing were performed using GeoDict software package (GeoDict 2018, Math2Market GmbH, Germany). 2D images were trimmed to a sub-volume (approximately 300× 300 × 300 microns) and filtered to remove noise. During the image segmentation process, the voxels of carbon and non-carbon species in the grayscale histogram were differentiated with the aid of OTSU-mediated threshold selection program. The resultant 3D reconstructed model was used to estimate the pore characteristics, such as porosity and pore diameter size distribution, using *PoroDict*® software package (*GeoDict*® 2018, Math2Market GmBH, Germany), where pore radius is determined by fitting spheres into the pore volume.

Numerical simulation of mass transport properties in xerogels was performed on their real 3D reconstructed model, using *FlowDict*® software package (*GeoDict*® 2018, Math2Market GmBH, Germany). Explicit jump solver was employed, which follows the *Stokes equation* and is ideal for application in flows when the flow velocity dependence is linear. The flow of water at 25 °C was simulated with a pressure drop of 20 Pa from all three directions (X, Y, and Z axis) of the real 3D structure. Iterations in the range of 300 to 850 were undertaken with a maximum error bound of less than 2 %. The average flow velocity fields were calculated by explicit jump solver in three directions by setting up the virtual pressure drop and selecting the computation directions or boundary conditions.

Section S-2: Synthetic Procedures and Methods

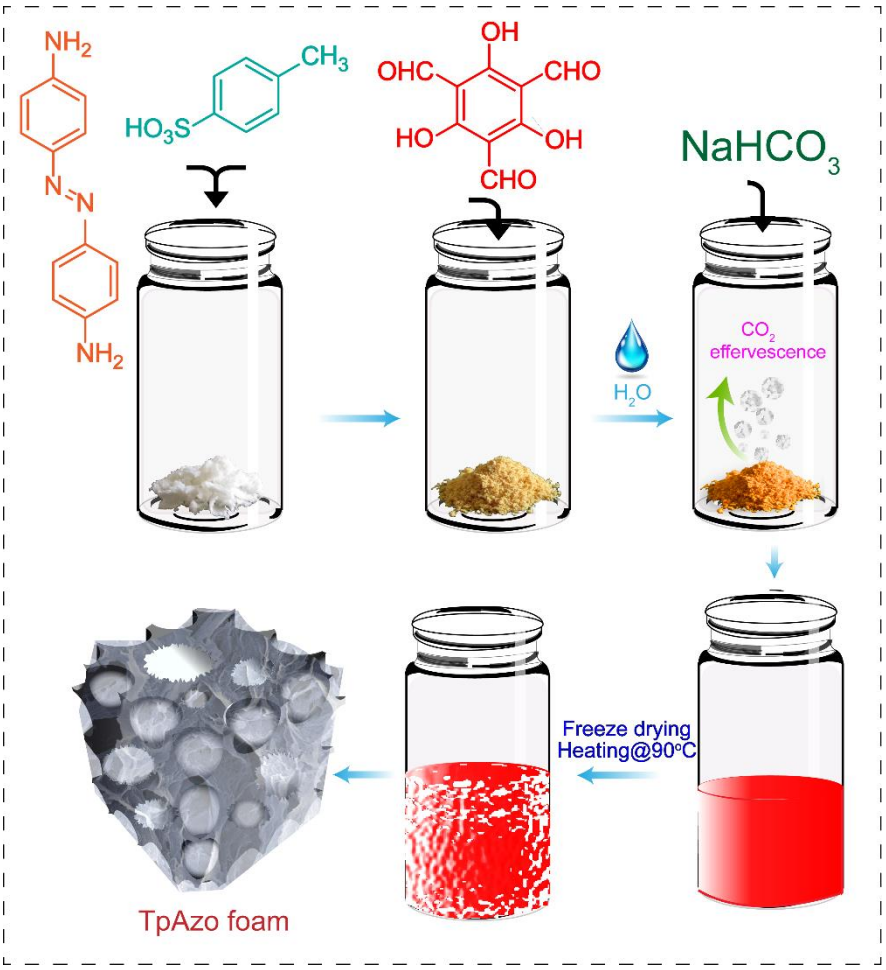

Figure S1. Synthetic scheme for the formation of TpAzo foam from the Tp aldehyde and Azo amine in the presence of excess PTSA with the help of CO_2 effervescences.

Synthesis of TpAzo COF-foam: 0.45 mmol of 4,4′-azodianiline (Azo) (95.5 mg) was added to a freshly dried 11.61 mmol of *p*-toluenesulfonic acid (PTSA), (2 g). The mixture was ground for 3-4 minutes to get a reddish powder-type texture. After that, 0.3 mmol of 1,3,5-triformylphloroglucinol (Tp) (63 mg) was added to the mixture and ground for 8 to 10 minutes. Around 100 µL of water was added to the mixture. It helped to form a paste-like material. Once the paste was formed 6 mmol of sodium bicarbonate ($NaHCO_3$), (500 mg) was added to the paste in a few portions and ground thoroughly. Few drops of water were added successively. The excess PTSA reacted with the sodium bicarbonate, resulting in in-situ CO_2 effervescences. The CO_2 effervescence turned the paste into a floppy substance and caused macropores in the COF crystallites (Figure S1). The resulting floppy material was freeze-dried for 8-10 h, followed by heating at 90 °C for 12 hours in a closed condition. Freeze drying helped to remove excess water keeping porous macrostructure intake. The resulting floppy material was washed with dimethylacetamide (DMAC) and water to remove the monomers and oligomers. It was dried at 120 °C for 12 h to get the TpAzo COF-foam.

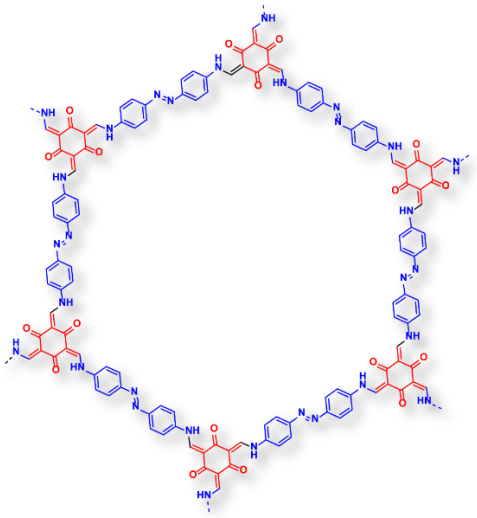

Figure S2. Chemdraw structure of TpAzo foam.

Section S-3: Enzyme expression and purification

Expression and Purification of proteins: The BGL, CBH, and EG genes were amplified, and a C-terminal 6-His tag was incorporated. All the genes were cloned into the pET-21b(+) expression vector and transformed into the Top10F′ Escherichia coli bacterial strain. A Qiagen Miniprep kit was used to isolate the plasmid, and the gene sequence was confirmed at the IISER Kolkata sequencing facility. Later, the plasmid was transformed into the BL21 bacterial strain of Escherichia coli (DE3).

All clones' initial cultures were cultured in LB media containing ampicillin (100 μg mL^{-1}) overnight at 37 °C with constant shaking (200 rpm). The overnight grown saturated solution was used to inoculate a 400 mL secondary culture by diluting in a ratio of 1 : 100. Protein synthesis was allowed for 6 hours at 37 °C after adding 0.5 mM IPTG to the culture to induce protein expression at an OD600 of 0.5-0.6. The cells were pelleted by centrifugation at 8000 rpm for 10 minutes at 4 °C and then kept at 20 °C until the protein was purified.

For protein purification, the cell pellet was thawed and resuspended in lysis buffer (10 mM potassium phosphate buffer, 10 mM imidazole, 500 mM NaCl, 1 mM PMSF, and 1.2 mg mL^{-1} lysozyme) at pH 7.4 and sonicated at 70% amplitude, 5 cycles of 1 min each with a 1 min interval between two consecutive cycles. Following a protocol previously reported,[3] the cell lysate was centrifuged at 13400 rpm for 15 minutes at 4 °C, and the clear supernatant was loaded onto a Ni–NTA column for purification. The purified proteins (BGL, CBH, and EG) were dialyzed in 10 mM HEPES (4-(2-hydroxyethyl)-1-piperazineethane sulfonic acid) buffer (pH 7.0),10 mM HEPES Buffer with 75mM NaCl (pH 6.0), and MES (2-(*N*-morpholino)ethane sulfonic acid) buffer (pH 6.0) and concentrated by 30 kDa cutoff-sized Amicon®-Ultra-15 membranes. The purity of all purified proteins was determined by performing 10% SDS-PAGE, and the protein concentration was determined by measuring the absorbance at 280 nm and using the extinction coefficient as per the modified Edelhoch and Gill/Von Hippel method available on the ExPASy ProtParam website by Swiss Institute of Bioinformatics.[4]

Section S-4: Enzyme Immobilization

Synthesis of BSA@TpAzo-foam: In a reaction tube, 1 mg of the oven-dried TpAzo foam was taken. 50 to 500 μL of a 4 mg/mL freshly prepared aqueous solution of Bovine serum albumin was poured into the reaction tube. The reaction mixture was then incubated at 4 °C for 2 h. After completion of incubation, the solution was centrifuged for 5 min at 13k rpm. 20 μL of the supernatant solution was diluted five times, and UV-vis absorbance was measured at 280 nm.

Synthesis of BSA@TpAzo-COF: In a reaction tube, 1 mg of the oven-dried TpAzo COF was taken. 50 to 400 μL of a freshly prepared aqueous solution of Bovine serum albumin (2 mg/mL) was poured into the reaction tube. The reaction mixture was then incubated at 4 °C for 2 h. After completion of incubation, the solution was centrifuged for 5 min at 13k rpm. 20 μL of the supernatant solution was diluted five times, and UV-vis absorbance was measured at 280 nm.

Synthesis of BGL@TpAzo-foam: 1 mg of TpAzo foam was placed in a reaction tube. In the tube, 50 to 400 µL of a freshly purified 4 mg/mL BGL enzyme in 10 mM HEPES (pH 7) buffer, was poured into the reaction tube. For 2 hours, the reaction mixture was allowed to incubate. The solution was centrifuged after the incubation, and UV-vis spectra of the supernatant were measured at 280 nm.

Synthesis of BGL@TpAzo-COF: 1 mg of TpAzo COF was placed in a reaction tube. In the tube, 400 µL of a freshly purified BGL enzyme in 10 mM HEPES buffer (pH 7) with a concentration of 4 mg/mL was poured into the reaction tube. For 2 hours, the reaction mixture was allowed to incubate. The solution was centrifuged after the incubation, and UV-vis spectra of the supernatant were measured at 280 nm.

Synthesis of CBH@TpAzo-foam: To immobilize CBH, 1 mg foam was taken in two reaction tubes separately. 50 to 400 µL of a prepared 4 mg/mL CBH solution in 10 mM HEPES buffer with 75 mM NaCl (pH 7) was added to the reaction tube. The mixtures were incubated for 2 h. Then the solutions were centrifuged, and the supernatant was separated to measure the UV-vis spectra at 280 nm.

Synthesis of CBH@TpAzo-COF: To immobilize CBH, 1 mg COF was taken in a reaction tube separately. 400 µL of a freshly prepared 4 mg/mL CBH solution in 10 mM HEPES buffer with 75 mM NaCl (pH 7) was added to the reaction tubes. The mixtures were incubated for 2 h. Then the solutions were centrifuged, and the supernatant was separated to measure the UV-vis spectra at 280 nm.

Synthesis of EG@TpAzo-foam: To immobilize EG, 1 mg foam was taken in two reaction tubes separately. 50 to 400 µL of a freshly prepared EG enzyme in 10 mM MES buffer (pH 6) with a concentration of 4 mg/ml was added to the reaction tubes. The mixture was incubated for 2 h. Then the solutions were centrifuged, and the supernatant was separated to measure the UV-vis spectra at 280 nm.

Synthesis of EG@TpAzo-COF: To immobilize EG, 1 mg COF was taken in two reaction tubes separately. 400 µL of freshly prepared EG solutions in 10 mM MES buffer (pH 6) with a concentration of 4 mg/mL was added to the reaction tubes. The mixtures were incubated for 2 h. Then the solutions were centrifuged, and the supernatant was separated to measure the UV-vis spectra at 280 nm.

Section S-5: Determination of the loading capacity of enzymes and leaching test

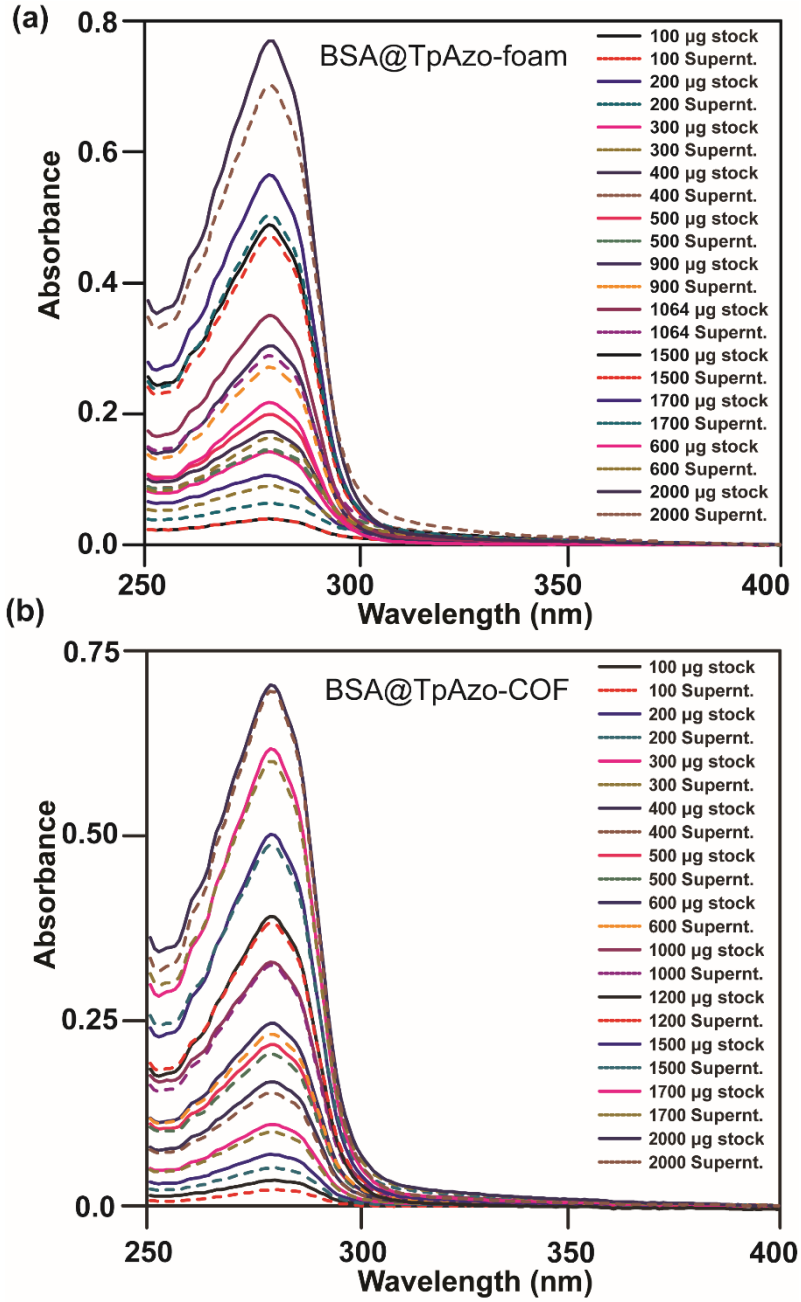

Figure S3. UV-vis absorption spectra of the stock solutions and supernatants after the loading of BSA in the TpAzo foam and COF.

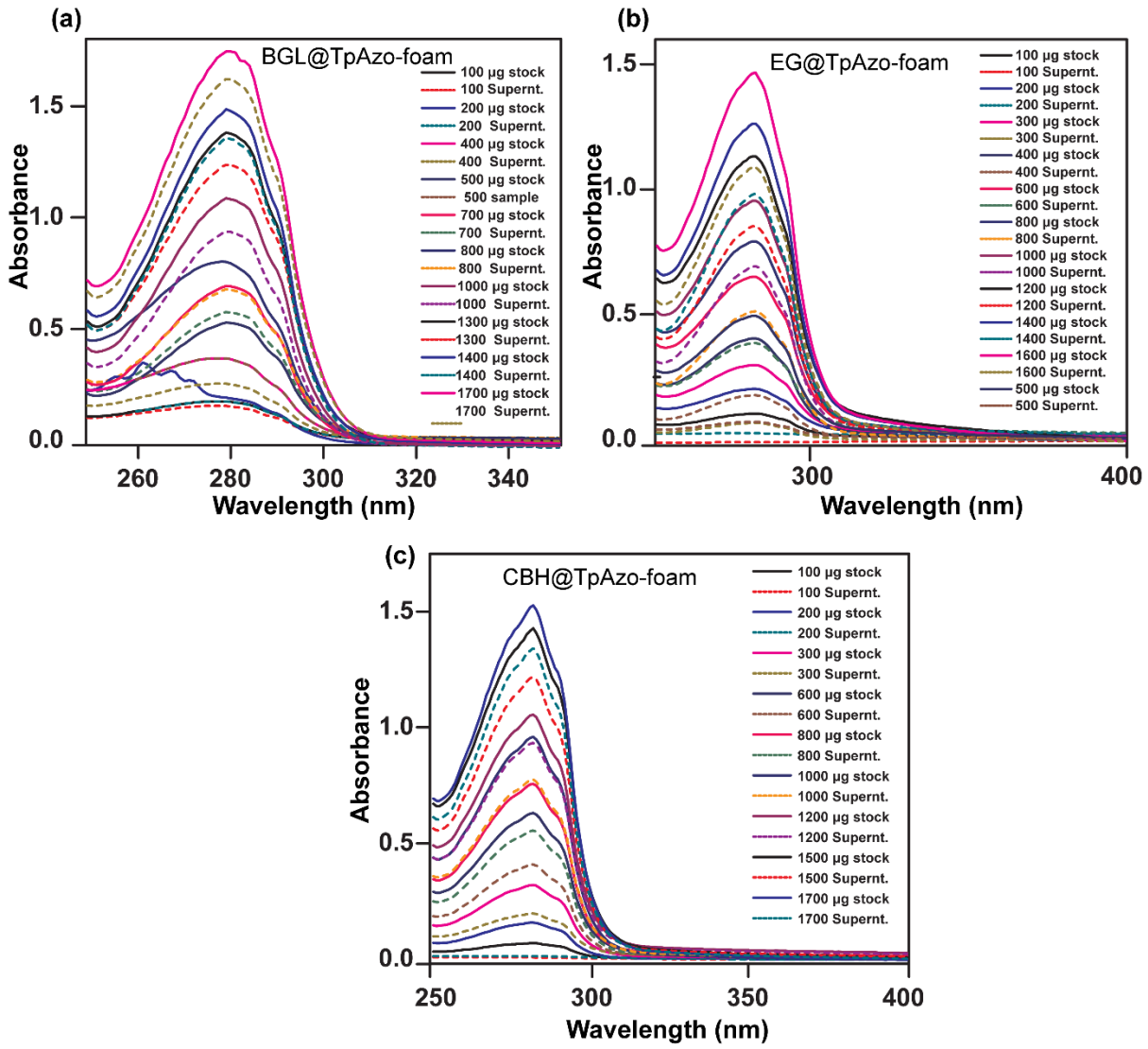

Figure S4. UV-vis absorption spectra of the stock solutions and supernatants after the loading of BGL,CBH, and EG with increasing stock quantity in the TpAzo foam.

To determine the adsorbed enzyme, the following procedure is maintained throughout all the experiments. After incubating the foam with a known enzyme concentration, the solution's final concentration was measured by the UV-spectroscopy of the supernatant. The adsorbed amount of enzyme at equilibrium was calculated by the following equation.

$$q_t = (C_0 - C_t) \times V, \qquad I_p(\%) = \frac{(C_0 - C_t) \times V}{m} \times 100$$

where q_t (µg) is the total adsorbed enzyme in the TpAzo foam (1 mg), I_p (%) is the adsorbed percentage of the enzyme, C_0 is the initial concentration of enzyme solution, C_t final concentration of enzyme solution, V is the volume of the treated solution (mL), m is the mass of the adsorbent (µg) TpAzo foam.

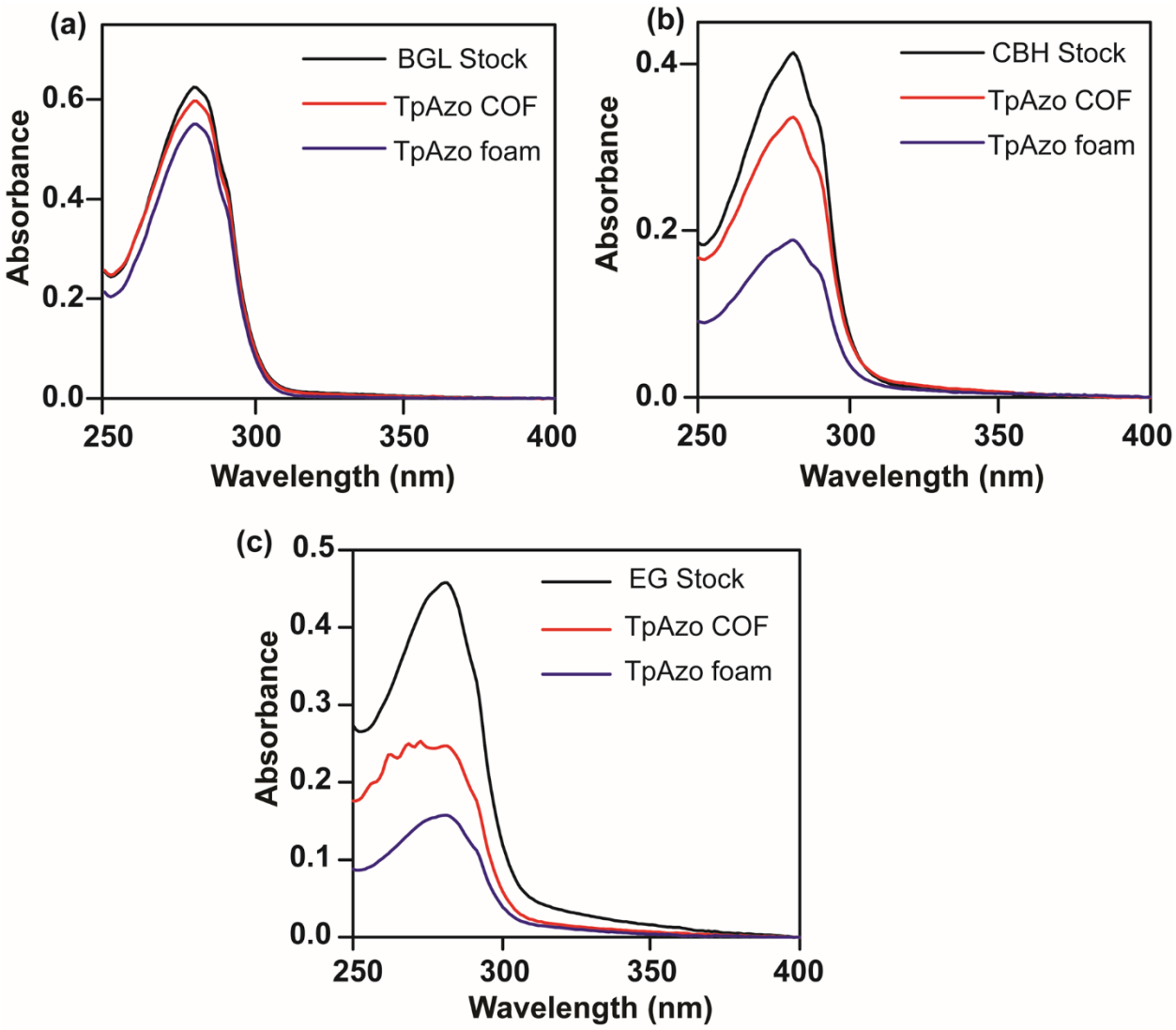

Figure S5. UV-vis absorption spectra of the stock solutions and supernatants after loading (a) BGL, (b) CBH, and (c) EG in the TpAzo COF and foam. From the absorbance value of the supernatants, the higher adsorption capacity of the enzymes in the foam compared to COF can be quantified.

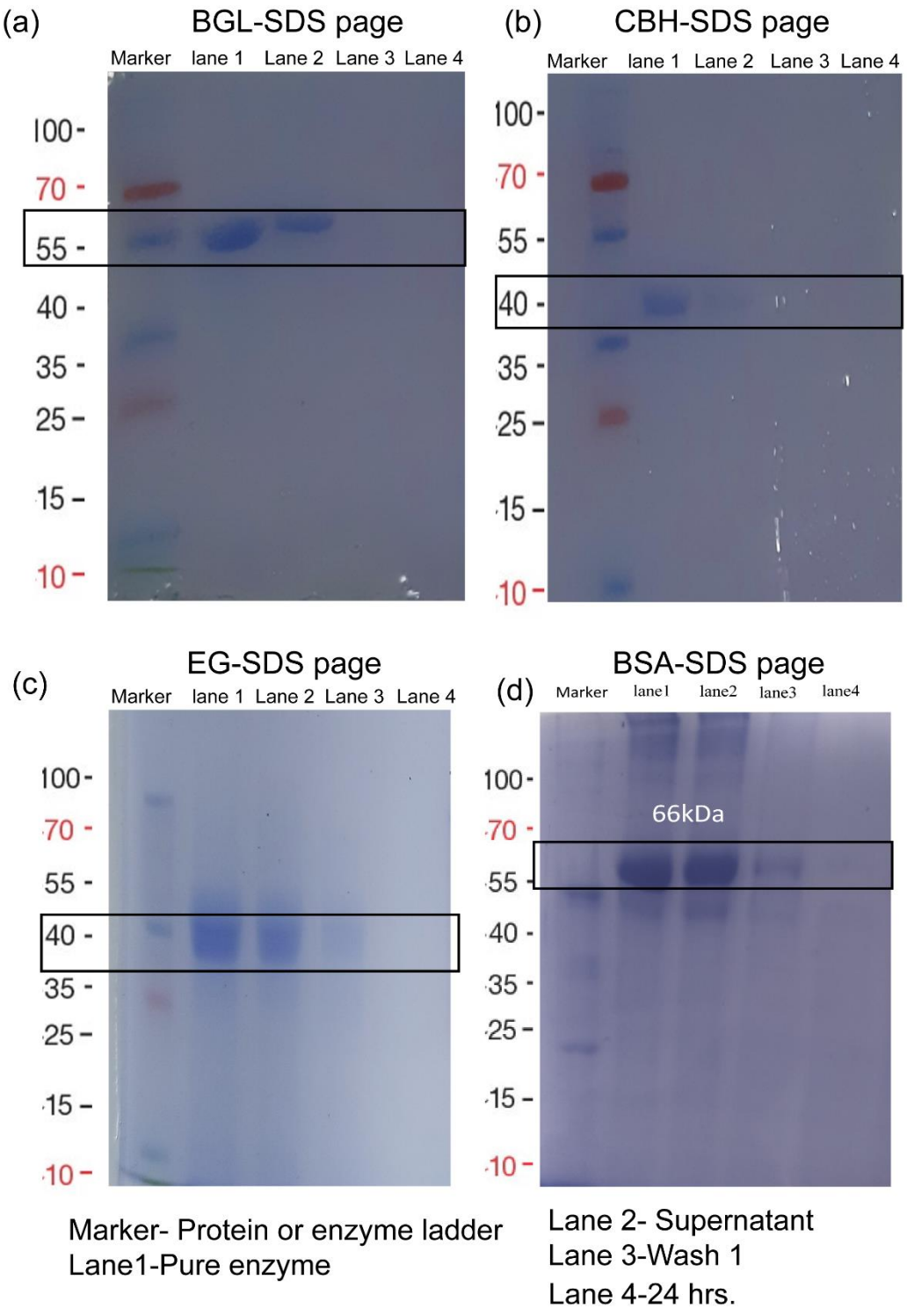

Figure S6. After adding enzymes to the TpAzo foam, an SDS page analysis of the supernatants and washed solutions was performed. The standard marker is in the first lane, and the second lane contains the supernatant solution after incubating the foam in the appropriate buffer solution. The third lane contains the first-washed solution of enzyme-loaded foams, and the fourth lane contains the supernatant after the enzyme-immobilized foam was kept in water for the SDS-PAGE.

Section S-6: Enzyme activity assay

pH optimization assay of the BGL@TpAzo-foam: The catalytic activity of the immobilized BGL@TpAzo-foam was determined using *p*-nitrophenyl-β-D-glucopyranoside (*p*NPGlc) as a substrate at different pH conditions. 10 µL of BGL@TpAzo-foam (equivalent to 0.5 µg of free BGL) were incubated with 90 µL of HEPES buffer of different pH (3-8) containing 40 mM of *p*-nitrophenyl-β-D-glucopyranoside (*p*NPGlc), at 70 °C for 5 min under 800 rpm shaking at Thermomixer. The reaction was stopped by adding 100 µL of stop solution (0.4 M glycine, pH 10.8). Then, the reaction product was diluted 20X, and absorbance was measured at 405 nm. The *p*NP generated was calculated by comparing it with a standard curve. A standard curve for 20X diluted *p*NP was recorded at 405 nm by adding 100 µL 10 mM HEPES buffer, pH 7.0, containing different concentrations of *p*NP (0.5, 0.75, 1.0, 1.50, 1.75, 2.0, 3.0, 4.0 mM) and 100 µL of stop solution (0.4 M glycine, pH 10.8).

Temperature optimization assay of the BGL@TpAzo-foam: The catalytic activity of the immobilized BGL@TpAzo-foam was determined on *p*NPGlc at different temperatures. 10 µL of BGL@TpAzo-foam (equivalent to 0.5 µg of free BGL) was incubated with 90 µL of 10 mM HEPES buffer, pH 7 containing 40 mM of *p*NPGlc at different temperatures (50, 55, 60, 65, 70, 80 °C) for 5 min under constant shaking at 800 rpm in a Thermomixer. The reaction was stopped by adding 100 µL stop solution (0.4 M glycine, pH 10.8). Then, the reaction product was diluted 20X, and absorbance was measured at 405nm. The *p*NP generated was calculated by comparing it with a standard curve.

Kinetics of BGL@TpAzo-foam: The catalytic activities and Michaelis-Menten constants (K_m) of the immobilized BGL@TpAzo-foam were determined on *p*NPGlc dissolved in 10 mM HEPES buffer, pH 7.0. The activity of the immobilized BGL@TpAzo-foam was measured. As this reaction follows zero-order kinetics (enzyme saturation), 10 µL of BGL@TpAzo-foam (equivalent to 0.5 µg of free BGL) were incubated with 90 µL of 10 mM HEPES buffer, pH 7.0 containing different concentrations of *p*NPGlc (1, 2, 5, 10, 20, 40, 50, 60, and 70 mM) at 70 °C for 5 min under constant shaking at 800 rpm on a Thermomixer. The reaction was stopped by adding 100 µL stop solution (0.4 M glycine, pH 10.8). Then, the reaction product was diluted 20X, and the absorbance was measured at 405 nm. The amount of product generated was calculated by comparing it to a standard curve.

Recyclability Assay for enzyme recycling: The recycled activity was measured on the chromogenic substrate, *p*NPGlc. For recycling assays, a 100 µL reaction mixture containing 10 µL of BGL@TpAzo-foam (equivalent to 0.5 µg of free BGL) and 40 mM of *p*NPGlc (final concentration) was incubated at 70 °C for 5 min with constant shaking at 800 rpm. To precipitate the BGL@TpAzo-foam, the reaction contents were centrifuged at 10000 rpm for 10 min, and the supernatant was decanted. The *p*NP in the supernatant was quantified by measuring absorbance at 405 nm by UV-visible spectrophotometry. The BGL@TpAzo-foam was reused for another product forming reaction up to ten cycles to compare the catalytic efficiency between the first and the later cycles.

pH optimization assay of the CBH@TpAzo-foam: The catalytic activity was determined on carboxymethyl cellulose (CMC) substrate, which is a cellulose derivative that contains carboxymethyl groups (-CH2-COOH) that are bound to some of the hydroxyl groups of the glucopyranose monomers that comprise the cellulose backbone, the average molecular weight of CMC is 90,000 (Sigma-Aldrich, St Louis, USA. CAS. 9004-32-4). The catalytic activity of the immobilized CBH@TpAzo-foam was determined on CMC at different pH. 10 µL of CBH@TpAzo-foam (equivalent to 0.5 µg of free CBH) were incubated 140 µL of McIlvaine buffer of different pH (3-8), containing 1 % CMC (10 mg/mL) at 55 °C for 15 min under 800 rpm shaking in a Thermomixer. Then 150 µL DNS reagent was added to the reaction mixture and incubated at 95 °C for 15 min. Then, the reaction mixture's absorbance was measured at 540 nm. The reducing sugars generated were quantified by comparing them to a DNS standard curve.

Temperature optimization assay of the CBH@TpAzo-foam: The catalytic activity of the immobilized CBH@TpAzo-foam was determined on CMC, at different temperatures. 10 µL of CBH@TpAzo-foam (equivalent to 0.5 µg of free CBH) were incubated with 140 µL of McIlvaine buffer, pH 6 containing 1% CMC(10 mg/mL) at 40, 50, 55, 60, 70, 80 °C for 15 min under 800 rpm shaking in a Thermomixer. Then 150 µL DNS reagent was added to the reaction mixture and incubated at 95°C for 15 min. The absorbance of the reaction mix was measured at 540 nm to quantitate the reducing sugar.

Kinetic Investigation of the CBH@TpAzo-foam: The catalytic activities and Michaelis-Menton constants (K_m) of the immobilized CBH@TpAzo-foam were determined on CMC. The activity of the immobilized CBH@TpAzo-foam was measured as the rate at which the CMC was hydrolyzed. Typically, 10 µL of CBH@TpAzo-foam (equivalent to 0.5 µg of free CBH) were incubated 140 µL of McIlvaine buffer, pH 6.0 containing different concentrations of CMC (2 to 26 mg/mL) at 55 °C for 15 min. Then 150 µL DNS reagent was added to the reaction mixture and incubated at 95°C for 15 min, and the reducing sugar was quantitated as detailed previously.

Recyclability Assay for enzyme recycling: The recycled activity was measured on CMC. For recycling assays, a 150 µL reaction mixture containing 10 µL of CBH@TpAzo-foam (equivalent to 0.5 µg of free CBH) and 1 % of CMC (10 mg/mL) was incubated at 55 °C for 15 min with constant shaking at 800 rpm on a Thermomixer. To precipitate the CBH@TpAzo-foam, the reaction contents were centrifuged at 10000 rpm for 10 min, and the supernatant was decanted for measuring reducing sugars, as detailed previously. The CBH@TpAzo-foam was reused for ten cycles to compare the catalytic efficiency between the first and the later cycles.

pH optimization assay of the EG@TpAzo-foam: The catalytic activity of the immobilized EG@TpAzo-foam was determined using CMC as a substrate at different pH conditions. 10 µL of EG@TpAzo-foam (equivalent to 0.5 µg of free EG) were incubated with 140 µL of McIlvaine buffer of different pH (3-8) contained 1% CMC (10 mg/mL) at 55 °C for 15 min under 800 rpm shaking at Thermo-mixer. Then 150 µL DNS reagent was added in the reaction mixture and incubated at 95°C for 15 min. Then, the reaction mixture's absorbance was taken at 540 nm. The generated product reducing sugars was calculated by comparing with DNS standard curve.

Temperature optimization assay of the EG@TpAzo-foam: The catalytic activity of the immobilized EG@TpAzo-foam was determined using CMC as a substrate at different temperature conditions. 10 µL of EG@TpAzo-foam (equivalent to 0.5 µg of free EG) were incubated 140 µL of McIlvaine buffer pH 6 containing 1% CMC (10 mg/mL) substrate at different conditions (40, 50, 55, 60, 70, 80 °C) for 15 min under 800 rpm shaking at Thermo-mixer. Then 150 µL DNS reagent was added in the reaction mixture and incubated at 95°C for 15 min. Then, the reaction mixture's absorbance was taken at 540 nm. The generated product reducing sugars was calculated by comparing it to a DNS standard curve.

Kinetic Investigation of the EG@TpAzo-foam: The catalytic activities and Michaelis-Menton constants (K_m) of the immobilized EG@TpAzo-foam were determined on CMC. The activity of the immobilized EG@TpAzo-foam was quantitated by DNS assay as previously explained. Typically, 10 µL of EG@TpAzo-foam (equivalent to 0.5 µg of free EG) were incubated 140 µL of McIlvaine buffer, pH 6.0 containing different concentrations of CMC (2 to 26 mg/mL) at 55 °C for 15 min under constant shaking at 800 rpm in a Thermomixer and the DNS assay as performed as detailed earlier. The generated product Reducing sugars was calculated by comparing to a DNS standard curve.

Recyclability assay for enzyme recycling: The recycled activity was measured on CMC. For recycling assays, a 150 µL reaction mixture containing 10 µL of EG@TpAzo-foam (equivalent to 0.5 µg of free EG) and 1 % of CMC (10 mg/mL) was incubated at 55 °C for 15 min with constant shaking at 800 rpm on a Thermomixer. To precipitate the EG@TpAzo-foam, the reaction contents were centrifuged at 10000 rpm for 10 min, and the supernatant was decanted. Then 140 µL DNS reagent was added to the supernatant and incubated at 95°C for 15 min. The reducing sugar generated was calculated by DNS assay as described previously. The EG@TpAzo-foam was reused for another product forming reaction up to ten cycles to compare the catalytic efficiency between the first and the later cycles.

One-Pot reaction assay: The glucose oxidase–peroxidase (GOD-POD) assay was used to measure the amount of glucose generated during the one-pot reaction. In one pot reaction, the substrate CMC was used. 100 µL reaction mixture containing 66.7 µL McIlvaine buffer (pH 6.0) 10 µL of EG@TpAzo-foam (equivalent to 0.5 µg of free EG), 10 µL of CBH@TpAzo-foam (equivalent to 0.5 µg of free CBH), 10 µL of BGL@TpAzo-foam (equivalent to 0.5 µg of free BGL) and 1 % CMC (10 mg/mL) was incubated at 55 °C for 30 min with constant shaking at 800 rpm on a Thermomixer. To precipitate the enzymes@TpAzo-foam, the reaction contents were centrifuged at 10000 rpm for 10 min, and the supernatant was decanted. The amount of glucose generated was measured by the glucose oxidase–peroxidase assay (Glucose Oxidase kit, Sigma-Aldrich, St Louis, USA) following the manufacturer's protocol.

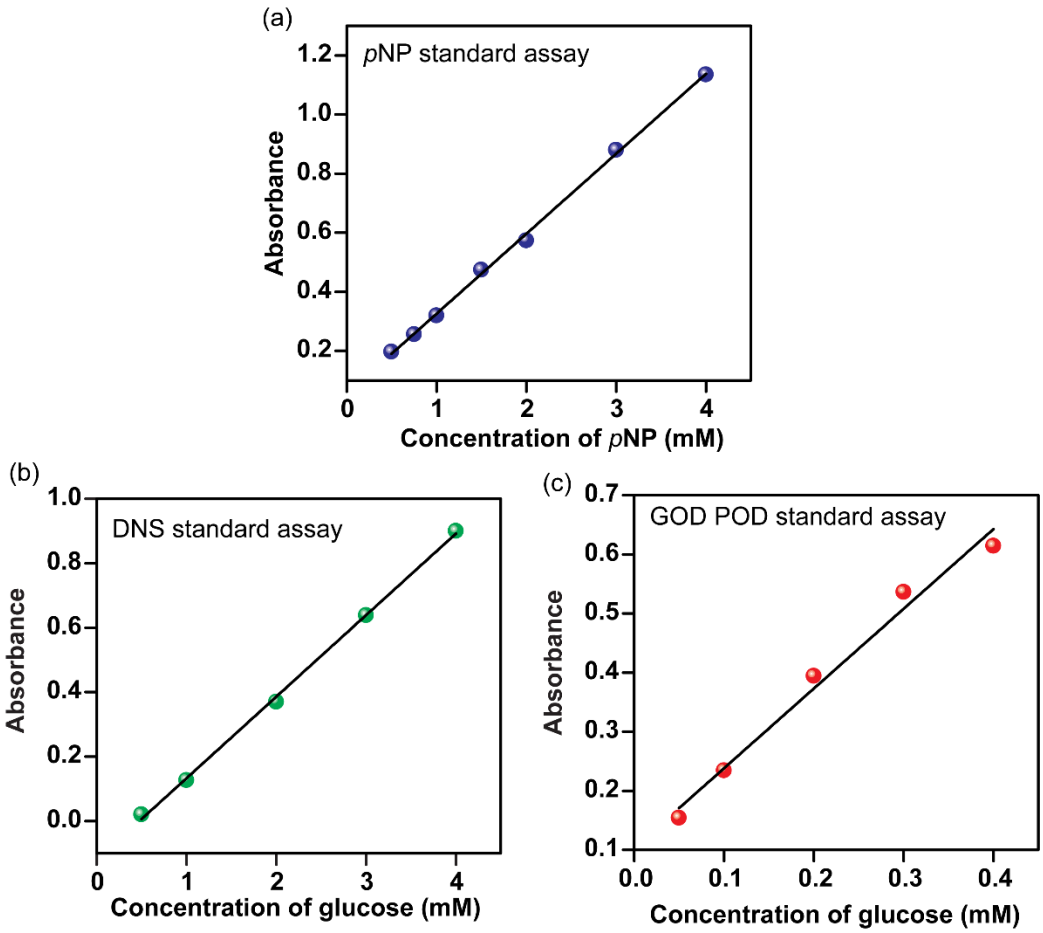

Figure S7. Standard curve of *p*NPGlc, DNS, and GOD POD assay.

Section S-7: SEM

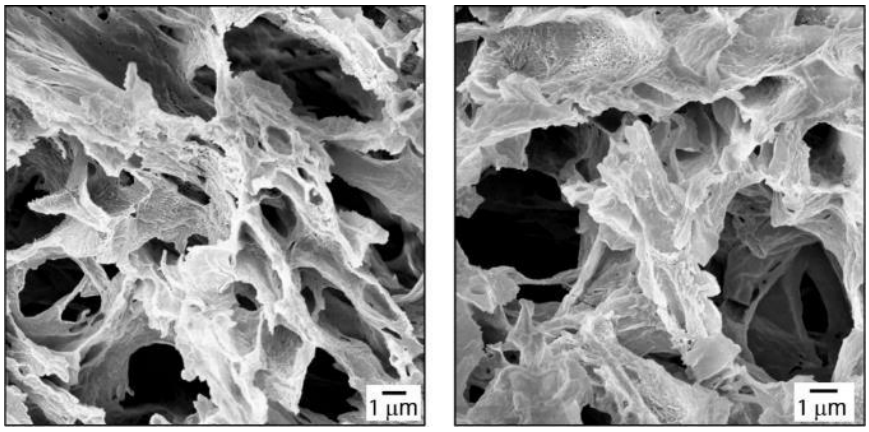

Figure S8. SEM images of TpAzo foam (1 µm) show disordered macro pores. The numerical value in the brackets represents the scale bar for the foam.

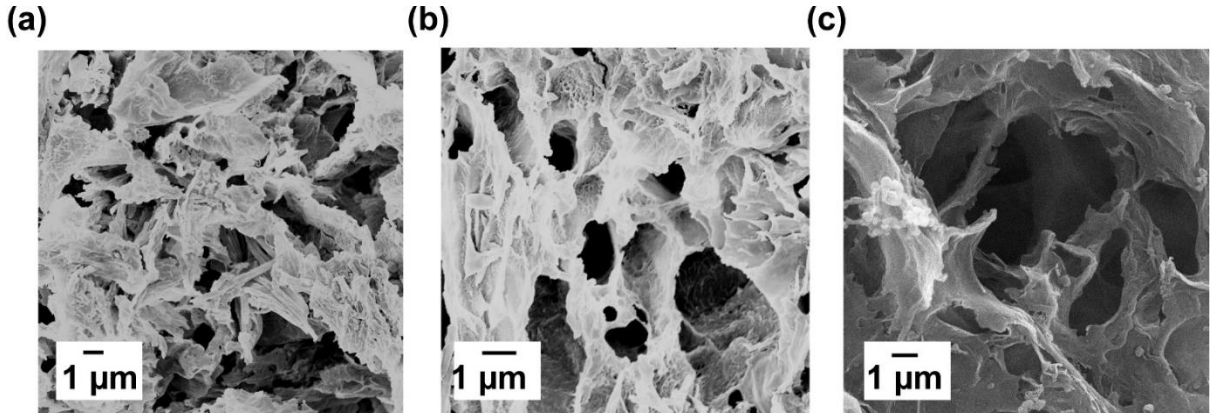

Figure S9. SEM images of (a) BGL@TpAzo-foam (b) CBH@TpAzo-foam (c) EG@TpAzo-foam.

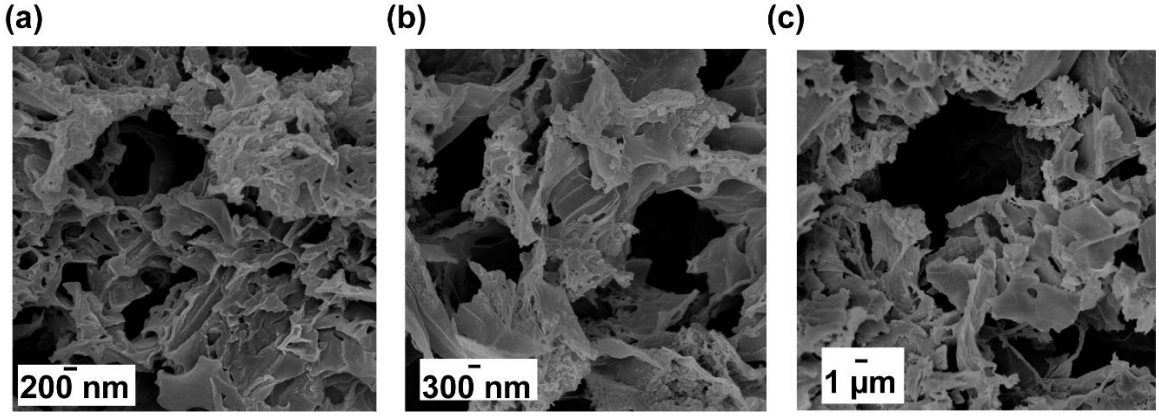

Figure S10. SEM images of (a) BGL@TpAzo-foam (b) CBH@TpAzo-foam (c) EG@TpAzo-foam after the 10 catalytic cycle**.**

Section S-8: TEM

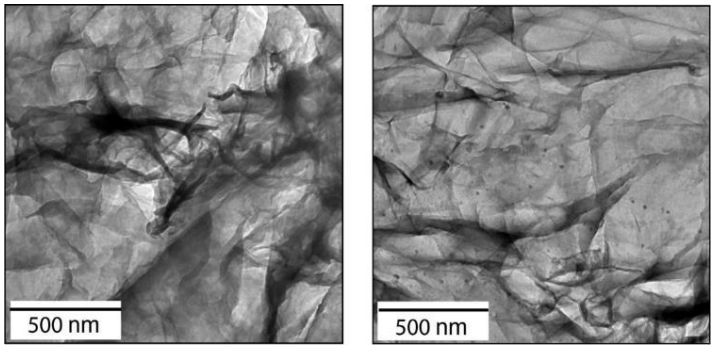

Figure S11. TEM images of TpAzo-foam (500 nm). The numerical value in the brackets represents the scale bar for the foam.

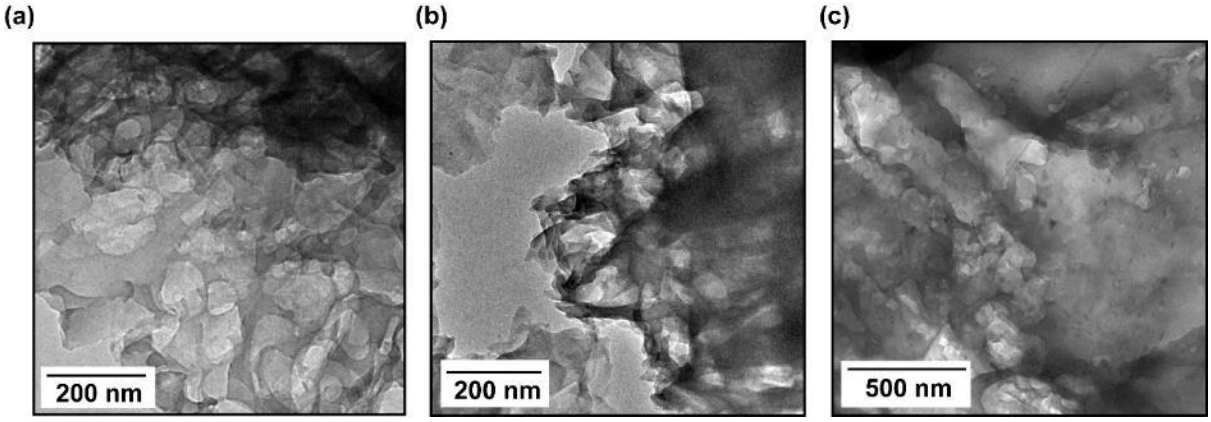

Figure S12. TEM images of (a) BGL@TpAzo-foam (b) CBH@TpAzo-foam (c) EG@TpAzo-foam.

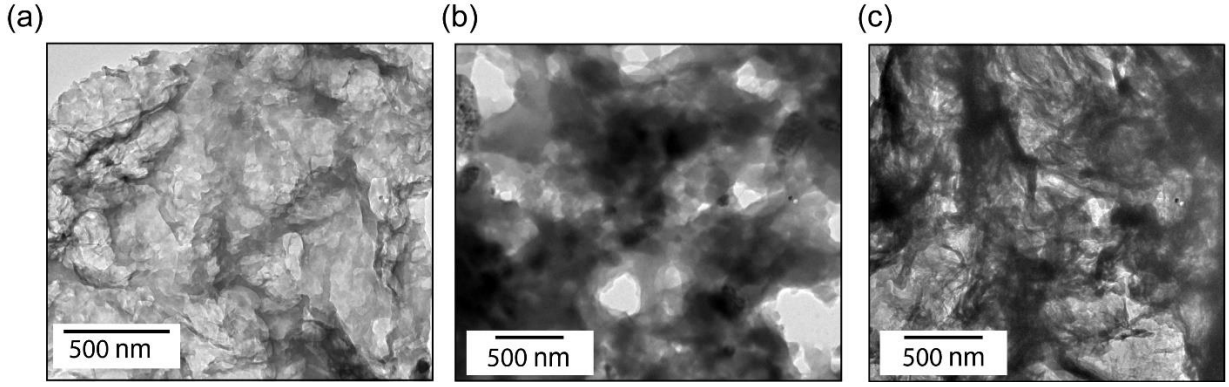

Figure S13. TEM images of (a) BGL@TpAzo-foam (b) CBH@TpAzo-foam (c) EG@TpAzo-foam after 10 catalytic cycle.

Section S-9: Confocal

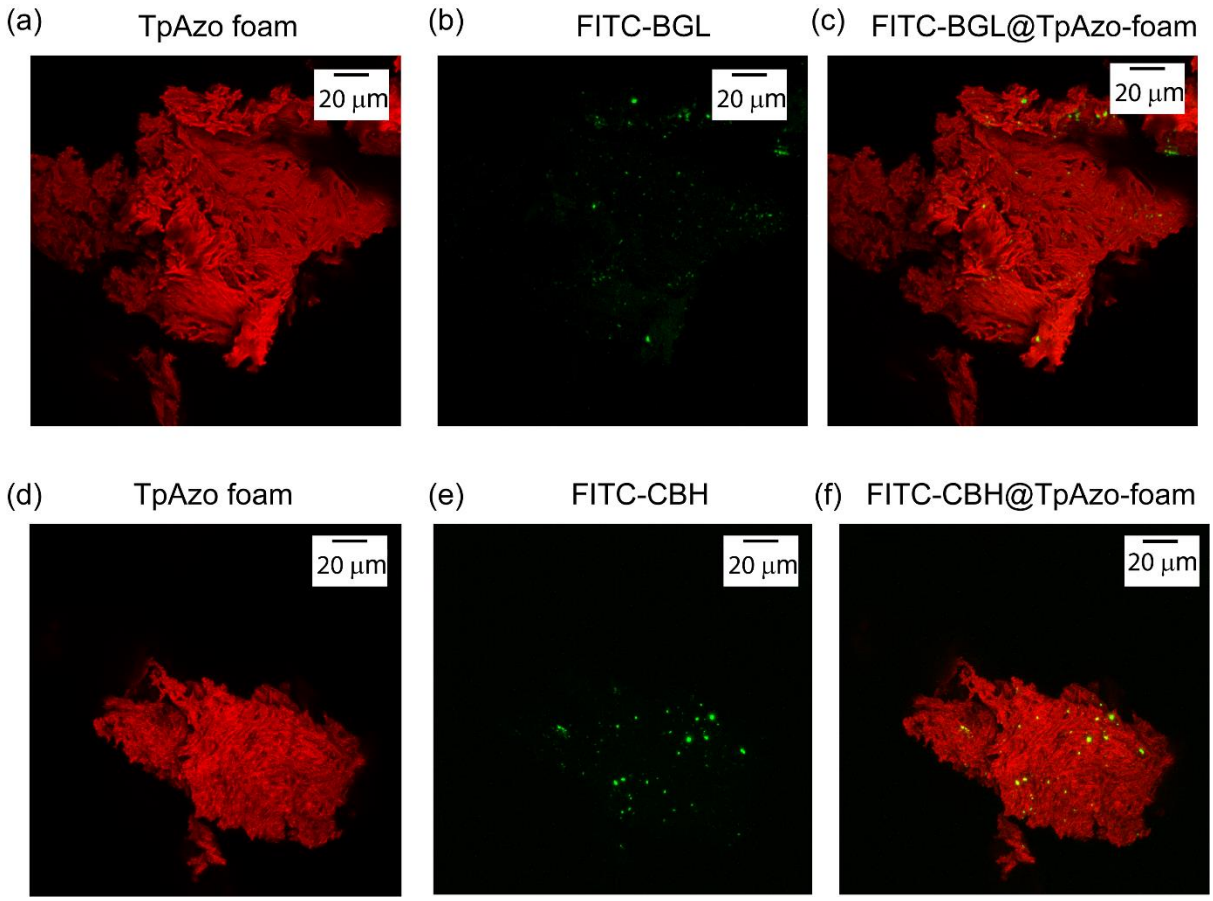

Figure S14. Confocal images of foam and enzyme-loaded TpAzo foam. (a,d): Confocal image TpAzo foam. (b) Confocal image of immobilized FITC-BGL (c) Overlay of a and b. (e) Confocal image of immobilized FITC-CBH. (f) Overlay of d and e

Section S-10: Structure Refinement

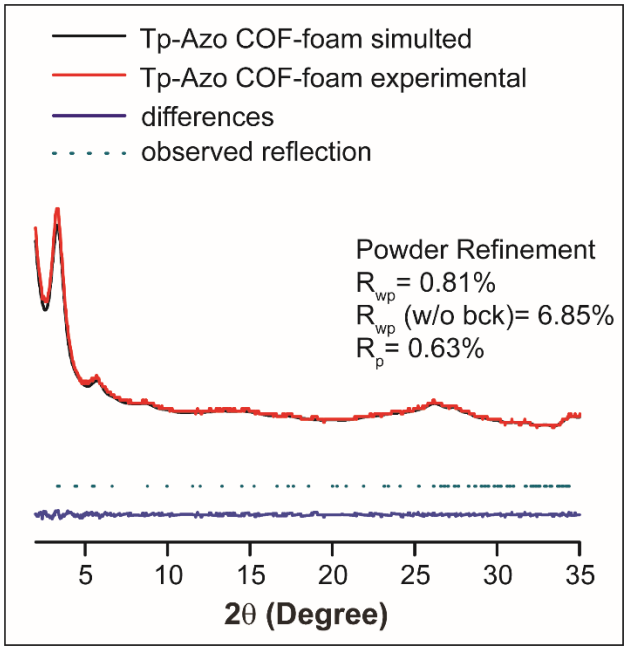

Figure S15. Pawley refinement PXRD patterns for TpAzo foam indicates that the experimental and modeled (eclipsed stacking) PXRD patterns match.

Table S1: Fractional atomic coordinates for the unit cell of TpAzo foam
TpAzo foam (Space group - P 6/m) a =31.50 Å, b= 31.50 Å, c=3.30 Å; α = 90º, β =90º, γ =120º

atoms	x	y	z
O1	0.29695	0.57697	0.00000
N2	0.38245	0.58505	0.00000
C3	0.31382	0.61757	0.00000
C4	0.39342	0.63145	0.00000
C5	0.41468	0.56990	0.00000
C6	0.46145	0.59947	0.00000
C7	0.49111	0.58277	0.00000
C8	0.47494	0.53664	0.00000
C9	0.42853	0.50701	0.00000
C10	0.39878	0.52354	0.00000
C11	0.36359	0.64675	0.00000
H12	0.42849	0.65656	0.00000
H13	0.47589	0.63531	0.00000
H14	0.34922	0.55946	0.00000
H15	0.36308	0.50007	0.00000
H16	0.52692	0.60571	0.00000
H17	0.41558	0.47120	0.00000
N1	0.50627	0.52081	0.00000

Section S-11: Nitrogen Adsorption Analyses

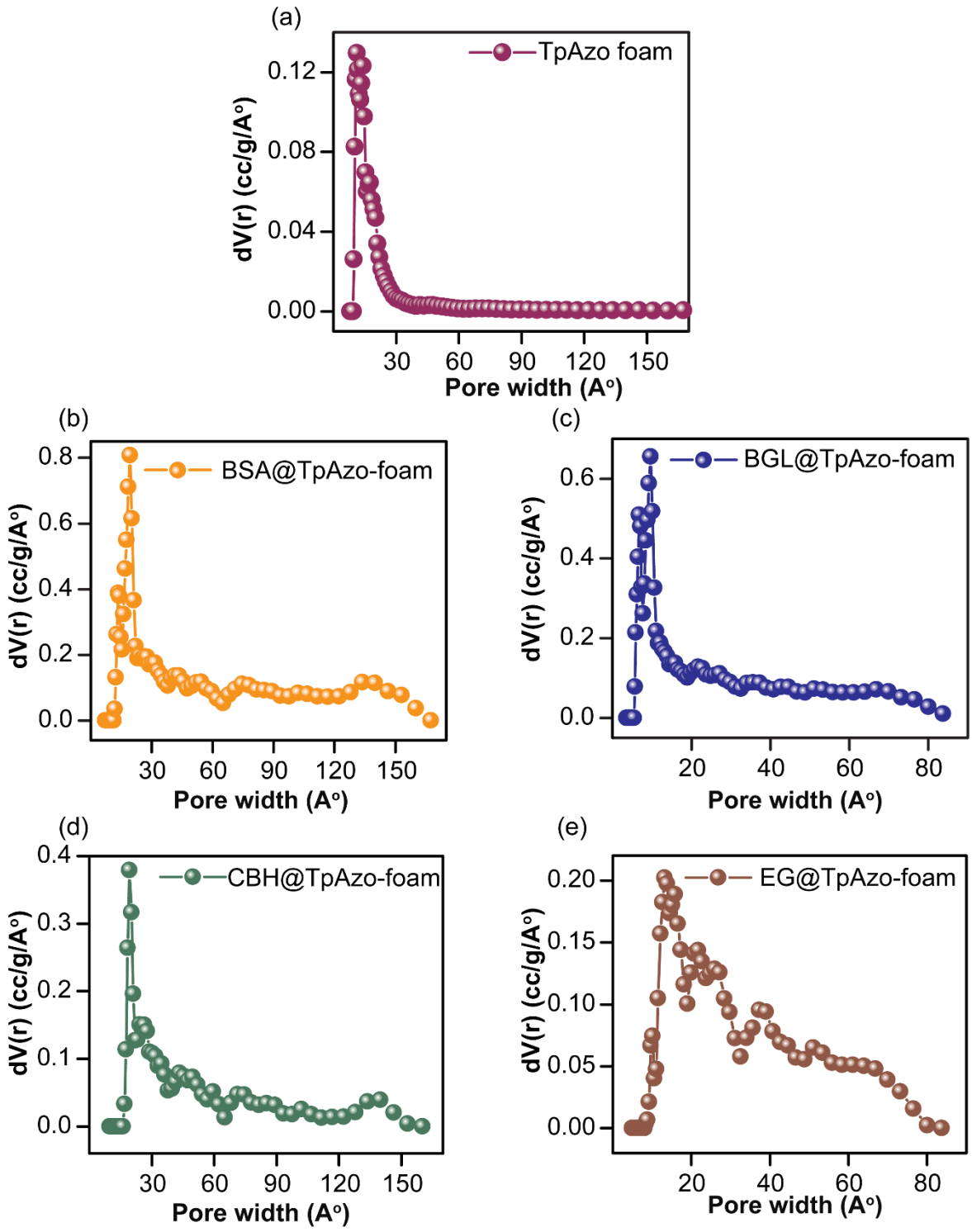

Figure S16. Pore size distribution of the TpAzo foam and enzymes immobilized foams. Pore size distributions of (a) TpAzo foam, (b) BSA@TpAzo-foam (c) BGL@TpAzo-foam (d) CBH@TpAzo-foam (e) EG@TpAzo-foam are showing unaltered micropore size distribution after the enzyme immobilization in the foam.

Section S-12: IR

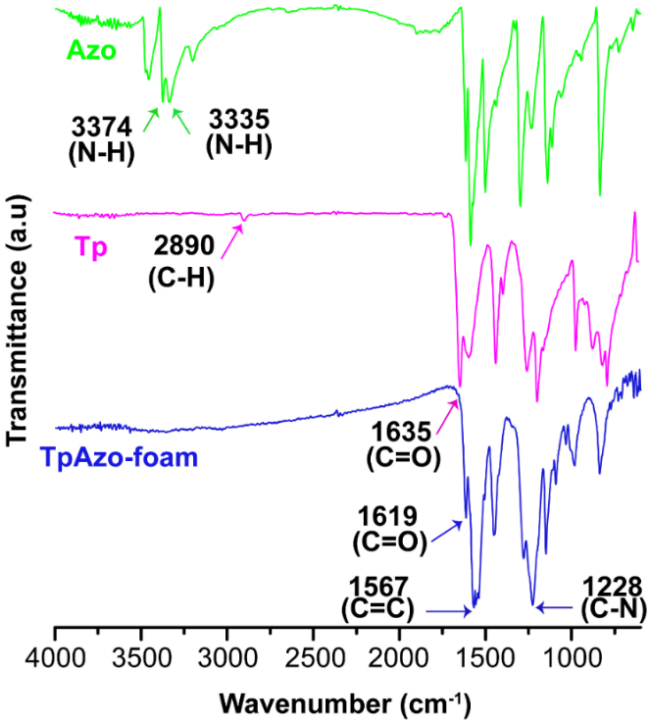

Figure S17. IR spectra of the starting materials Tp (1,3,5-triformylphloroglucinol) and Azo (4,4′-azodianiline) and the as-synthesized TpAzo foam.

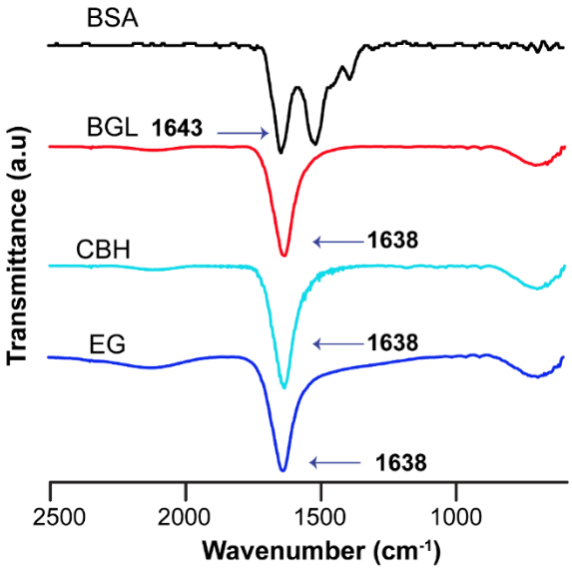

Figure S18. IR spectra of BSA, BGL, CBH, and EG.

Section S-13: X-ray microtomography analysis

Estimation of Pore Surface Area: The algorithm used to estimate specific (pore) surface area calculates an approximation of the surface area by statistical methods. To determine the surface area, the Crofton Formula[5] is used, which relates the 3D surface area to an integral over 2D boundary lengths of planar cross sections and then second these lengths to an integral over 1D rays. Based on this formula, analyzing the intersection points of rays in all space directions with the structure allows for determining the surface area.

Determination of Porosity: Samples were scanned at a specific pixel size during the X-ray micro-tomography imaging process, and the size depends upon the resolution. Scanned virtual cross-sectional images were subjected to an image processing technique called segmentation, where pixels pertaining to pore space were differentiated. During this process, porosity was calculated. Thereafter, the total pore volume was defined and divided by the total sample volume. The pore radius was determined by fitting spheres into the pore volume. A point belongs to a pore of radius larger than *r*, if it is inside any sphere of radius *r*, which can be fitted into the pore space.

$$Porosity\ (\%) = \frac{Pore\ Volume}{Total\ Volume}\ x\ 100$$

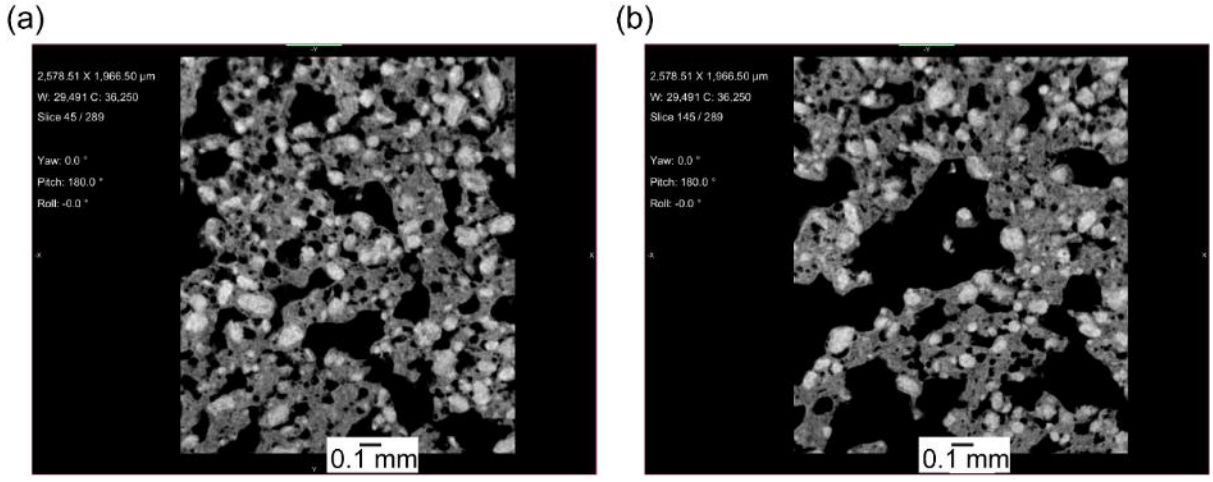

Figure S19. The cross-sectional two-dimensional tomography images of the TpAzo foam.

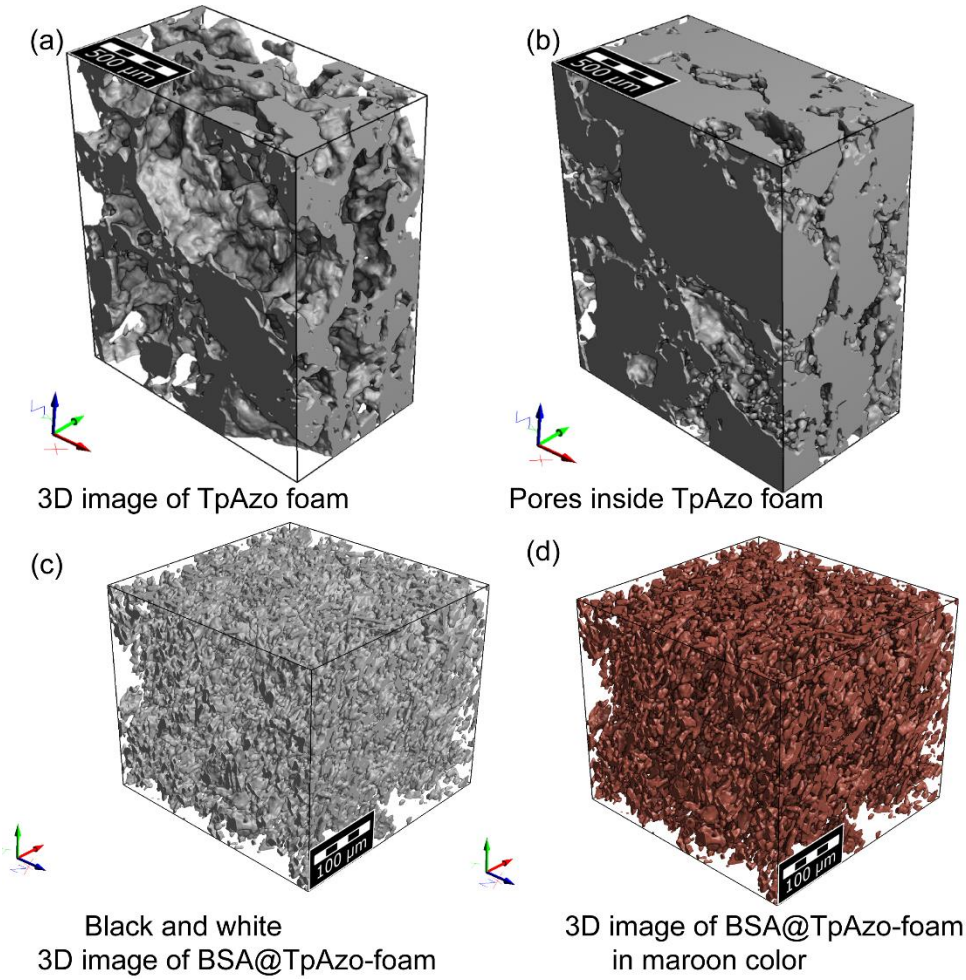

Figure S20. The X-ray tomography 3D images of (a) 3D image of foam (b) Pores inside foam (c) Black and white 3D image of BSA@TpAzo-foam (d) 3D image of BSA@TpAzo-foam in maroon color.

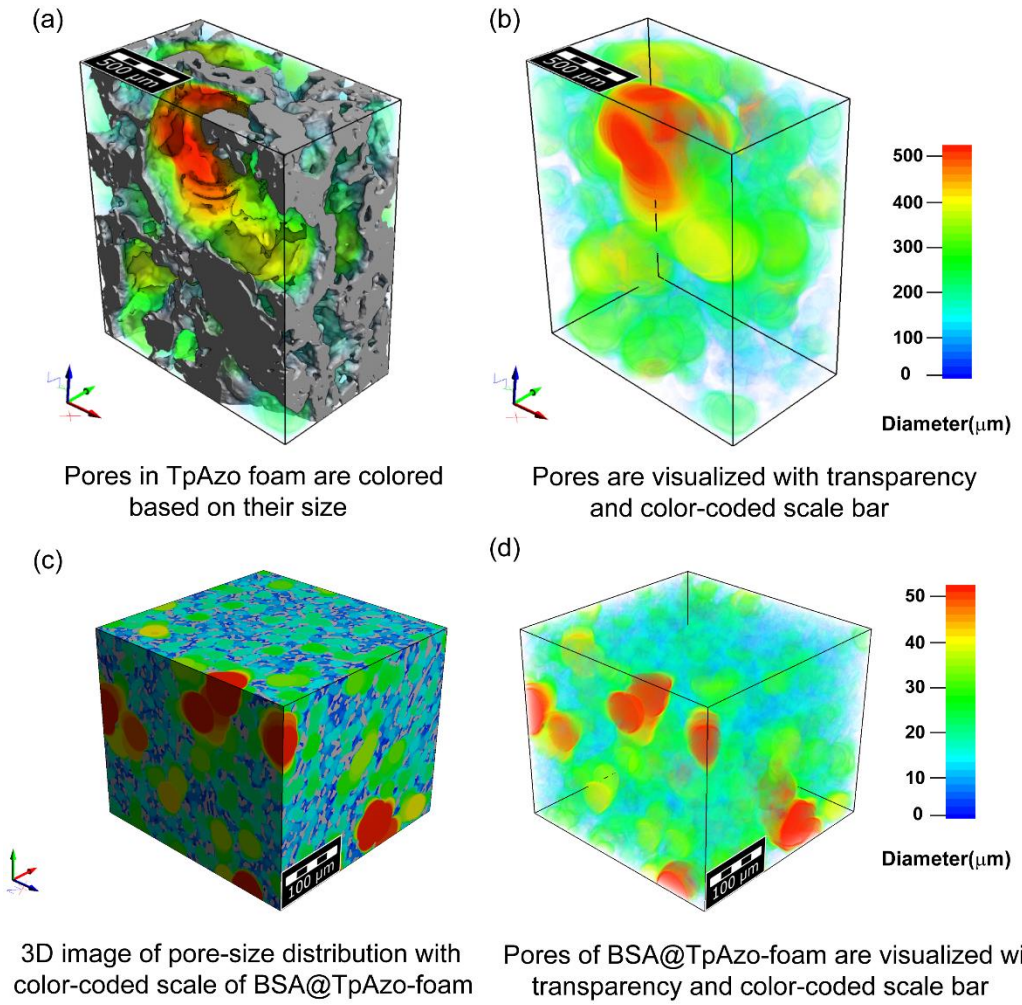

Figure S21. The 3D visualization of pore size distribution in TpAzo foam and BSA@TpAzo-foam from the X-ray tomography analysis. To study the pore characteristics of foams, tomography images were segmented to calculate porosity, and appropriate models were fitted onto the pore volume to estimate their size distribution. Resultant pore volumes are colored and scaled based on their size (a) Pores in TpAzo foam are colored based on their size. (b) Pores of TpAzo foam are visualized with transparency and a color-coded scale bar (c) 3D image of pore-size distribution with a color-coded scale. Both foam (grey color) and pores of BSA@TpAzo-foam are shown (d) Pores of BSA@TpAzo-foam are visualized with transparency and color-coded scale bar.

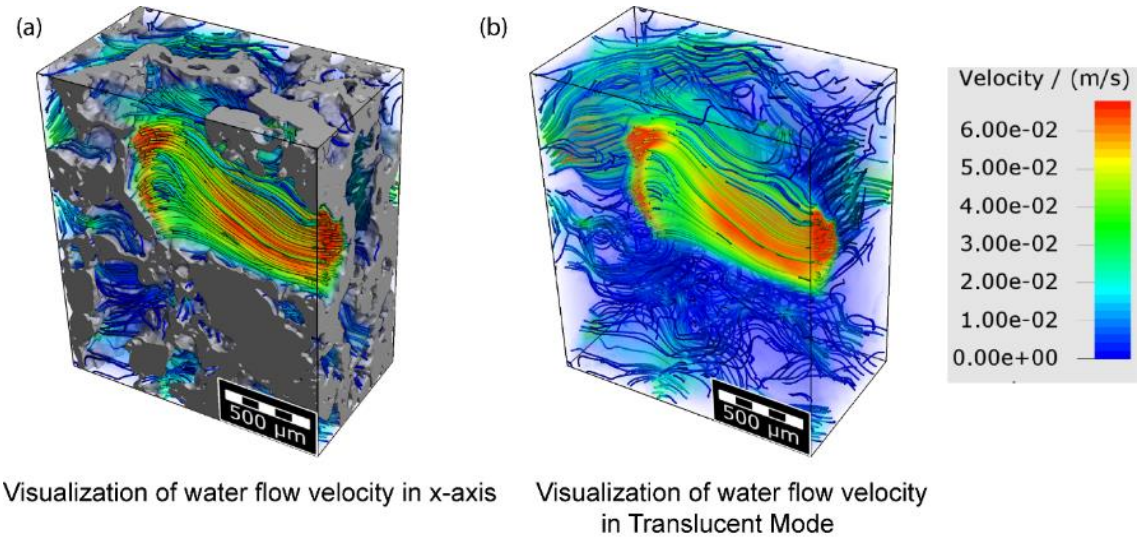

Figure S22. 3D visualization depicting the outcome of numerical simulation experiments performed on real 3D data volume of TpAzo foam. (a) 3D visualization of the flow velocity profile of water through inter-connected pore networks inside TpAzo foam and (b) visualization of flow streamlets connecting the pore networks with transparency.

Section S-14: Optimization of enzyme assay

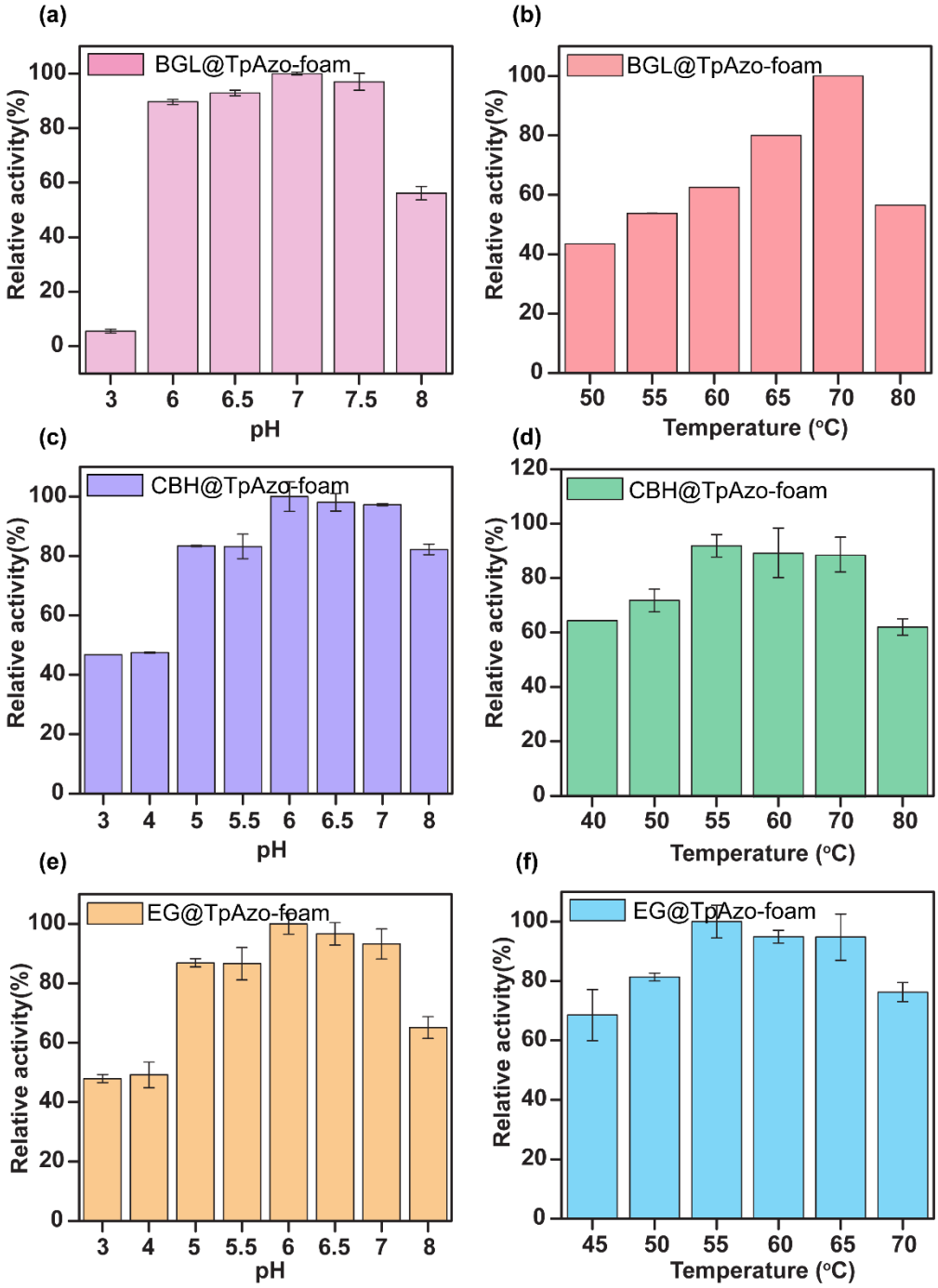

Figure S23. Optimization of pH and temperatures to check the activity of BGL, CBH, and EG in TpAzo foam. (Error bars in S21 b are invisible due to the short-range error bar)

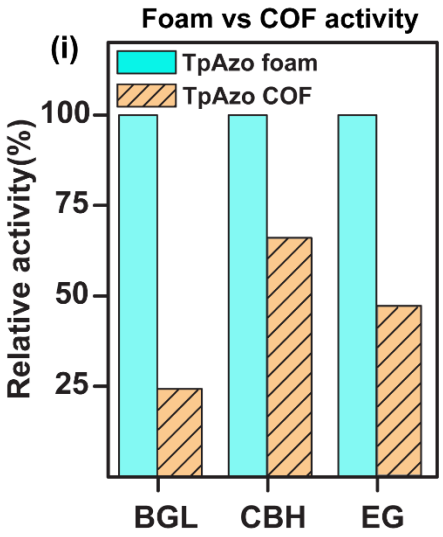

Figure S24. Comparison of the relative activity of BGL, CBH, and EG in TpAzo COF vs. TpAzo foam.

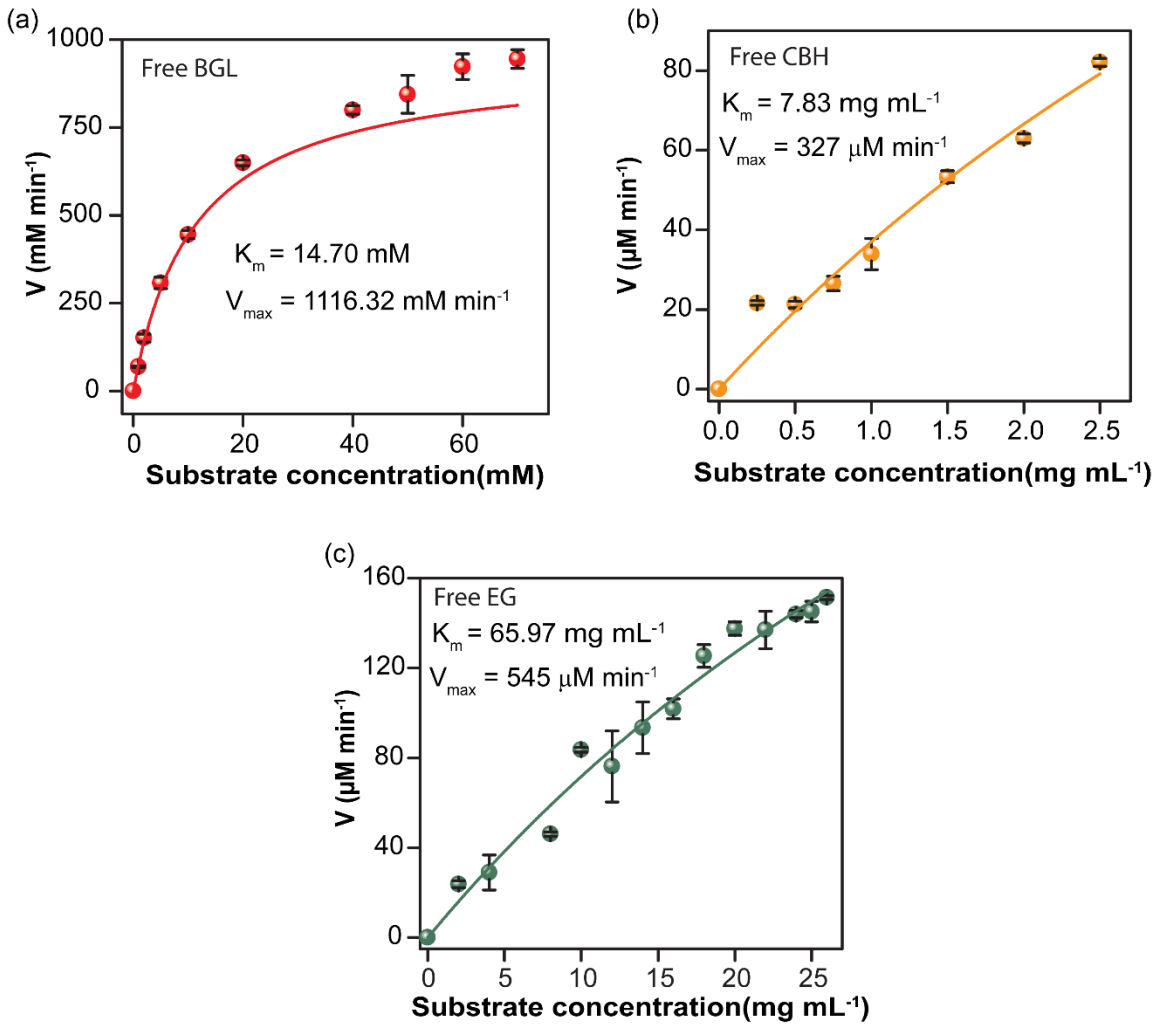

Figure S25. Michaelis-Menten plot of free BGL, CBH, and EG.

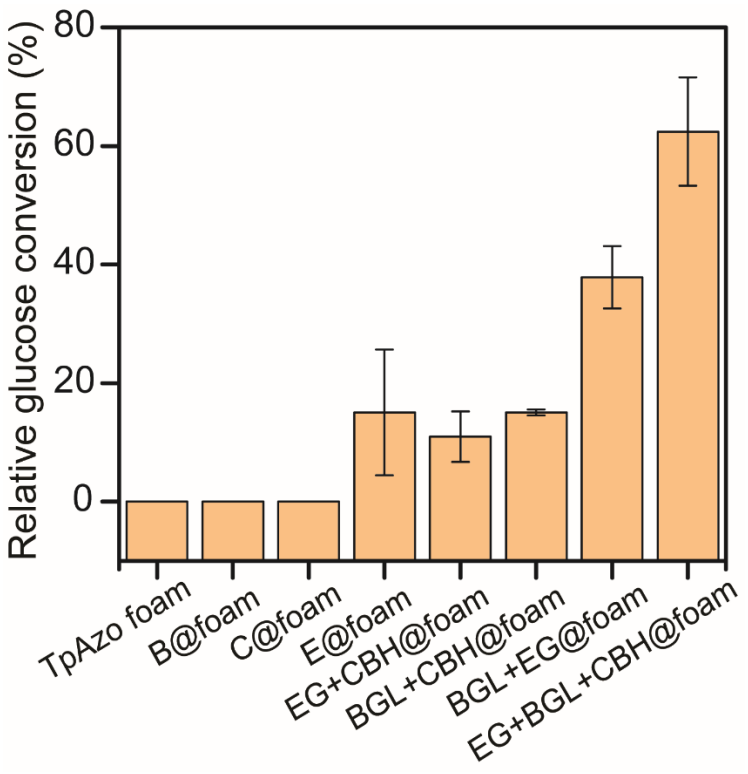

Figure S26. The relative conversion of CMC is catalyzed by the simultaneously immobilized enzymes (BGL+CBH+EG@TpAzo-foam) in the foam. (B: BGL, C: CBH, E: EG)

Section S-15: Molecular Dynamics Simulation

All calculations were performed using the Amsterdam Modelling Suite by Software for Chemistry and Materials (SCM-AMS).[6] The computations were started with the construction and optimization of a monolayer of TpAzo foam using the GFN-xTB (Geometry, Frequency, Non-covalent, Extended Tight Binding) method with relaxed lattice parameters and without any geometry constraint.[7] The GFN-xTB method is a computationally robust tight-binding semi-empirical method that was developed for computing molecular properties with higher accuracy for elements up to $Z \leq 86$ across the periodic table. From the optimized monolayer, a 4-layer AA-stacked TpAzo foam was modelled with a 4×4 unit cell (a=132.98 Å, b=132.98 Å) (Fig. S25) in order to evaluate the noncovalent intermolecular interaction between guest enzyme molecules and TpAzo foam. The large supercell ensured enzymes did not interact with their images in the 2D periodic system. The calculated average separations ($D_{E\text{---}E}$) between enzyme molecules in periodic systems are 65.95, 78.03, and 85.73 Å for BGL@TpAzo-foam, CBH@ TpAzo-foam, and EG@ TpAzo-foam, respectively (see Table S2 for more detail).

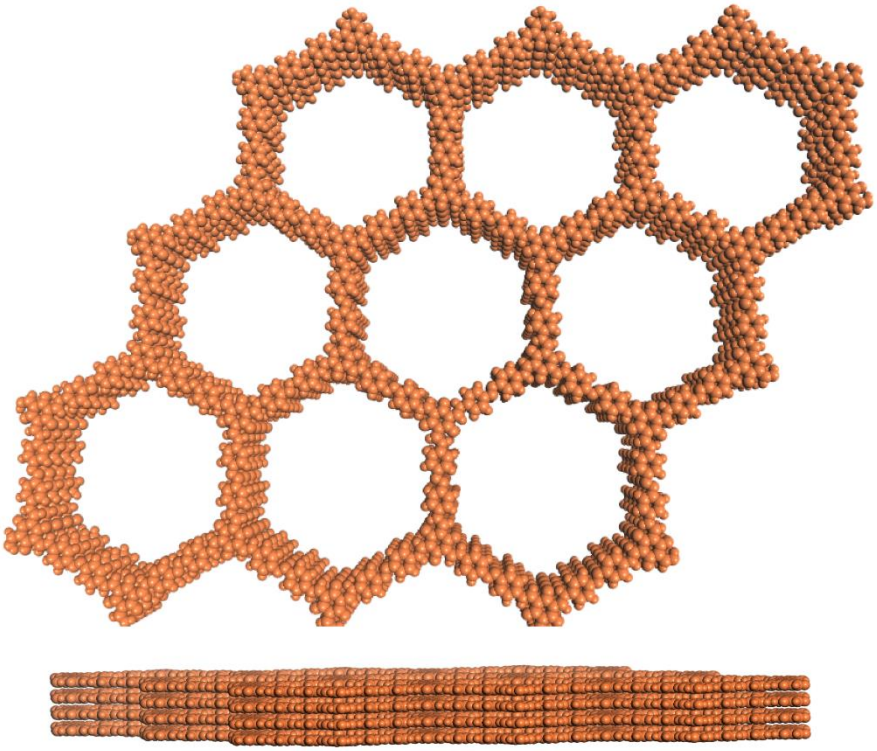

Figure S27. Top and side structure representation of 4x4 unit cell of TpAzo foam with interlayer separation of 3.39 Å.

Although, Quantum Mechanics (QM) methods are typically recommended for the prediction of free energy or the interaction energies in large molecular systems including biomolecules and supramolecular assemblies.[8] However, even semi-empirical QM methods are computationally too expensive for the ~10k atom enzyme@TpAzo-foam systems under study here. Therefore, prior to QM calculations, the interaction geometries of three different enzymes e.g., BGL CBH, and EG onto the TpAzo foam were investigated using Molecular Dynamics simulations using the Universal Force Field in order to reduce the computational cost.[9] Initially, the five different interaction geometries of each enzyme were set manually on the TpAzo foam, subsequently, the

systems were equilibrated at 298 K temperature using a global Nosé-Hoover thermostat for 2×10^5 steps, where the time steps for MD simulations were set to be 0.25 fs.[10] During the MD calculations, the bottom two layers of TpAzo foam were held fixed in order to maintain stacking interactions between the TpAzo foam layers, which prevents the top two layers from extensive deformation but permits interaction with the enzymes.

To calculate interaction energies, the final snapshots of each MD run were calculated using a hybrid strategy known as Quantum Mechanics/Molecular Mechanics (QM/MM) approach in order to measure the accurate interaction energies between guest enzyme molecules and TpAzo foam with the lowest computational cost. The hybrid QM/MM approach was first developed by Morokuma *et al*. in the 1990s approach enables two different methods to be applied to different parts of a large molecular system and combined to produce consistent numeric energies.[11] The QM/MM calculations were performed via a Hybrid Engine in SCM-AMS. In setting up QM/MM calculations, the interacting atoms (within the region of 15 Å from the top layer of TpAzo foam toward enzymes) of the enzyme-foam (E_n@TpAzo-foam where *n* represents three different enzymes) system were defined as a separate region and computed with the fast DFTB-QM method (GFN-xTB), and UFF was applied to the remaining atoms.

A total of fifteen structures were computed for three enzymes with the TpAzo foam. The noncovalent intermolecular interaction energies (E_{int}) between enzymes and TpAzo foam were computed using the expression below, which was accomplished by performing single-point QM/MM energy calculations for E_n@COF and their individual members (i.e., E_n and TpAzo foam).

$$E_{int} = E_{En@\ TpAzo\text{-}foam} - (E_{En} + E_{TpAzo\ foam})$$

Lastly, the surface area and volume of large enzyme molecules are computed using a 1.86Å (N_2) probe in Zeo++ software.[12] The calculated enzyme surface areas and volumes occupied by BGL, CBH, and EG are shown in Table 2.

Table S2. Surface areas and volumes of enzymes.

Enzyme	Surface Area ($Å^2$)	Volume ($Å^3$)
BGL	16240	97880
CBH	13565	74660
EG	15489	82340

Results and Discussion:

The interaction energies of three enzymes with five conformers each at QM/MM with DFTB/UFF are computed and structures are given in Table 3 and (Figures 28-30) for BGL, CBH, and EG, respectively. In the case of BGL, the maximum interaction stability is attained for the BGL@TpAzo-foam_5 structure with the E_{int} of -554.47 kJ mol^{-1}, followed by the structure BGL@TpAzo-foam_4 with the E_{int} of -349.53 kJ mol^{-1}. In the structures BGL@TpAzo-foam_5 and BGL@TpAzo-foam_4, the enzyme molecules interact closely with the two layers of TpAzo foam. The closest interaction distances ($D_{int/s}$) between BGL and TpAzo foam atoms are 2.56 Å in both structures 4 and 5. Unlike structure 4/5, the enzyme adsorbs onto the surface of TpAzo foam in BGL@TpAzo-foam_2 and BGL@TpAzo-foam_3 structures, thus the number of H-bonds reduces. H-bonding plays an important role in adsorbing biological molecules i.e., amino acids and nitrogenous bases. Owing to the ≥7 H-bonds between BGL and TpAzo foam atoms, the BGL@TpAzo-foam_5 exhibits the highest stability. As the number of H-bonds decreases the interaction stability also decreases. The interaction energies of BGL@TpAzo-foam _3 and BGL@TpAzo-foam_2 increase to -164.58 and -131.62 kJ mol^{-1}, respectively. However, the lowest

interaction energy is observed for the BGL@TpAzo-foam_1 structure (-93.51 kJ mol^{-1}) along with the largest interaction distance (3.66 Å), which is not within the typical range of H-bonds, which manifests the lowest stability of this conformation.

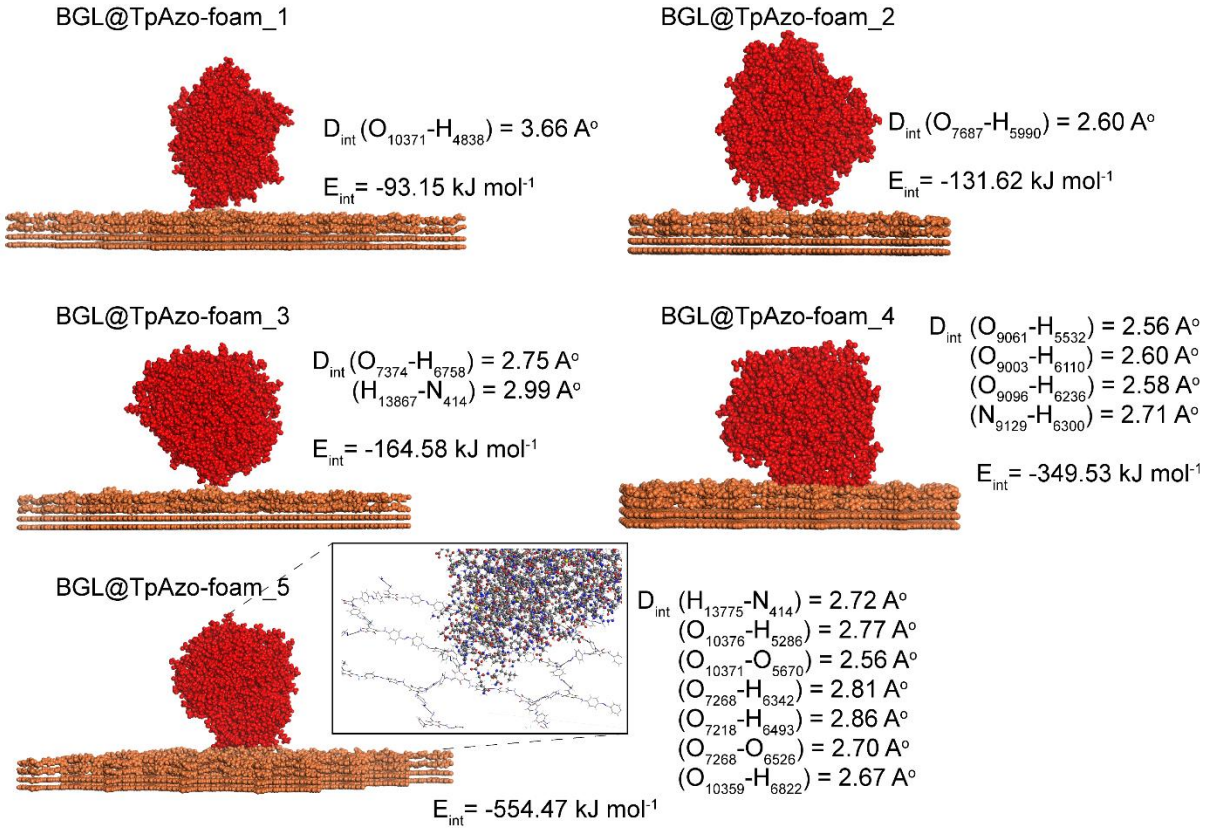

Figure S28. Five interaction geometries of BGL and TpAzo foam.

Similarly to the BGL@TpAzo-foam structures, the highest negative interaction energy is observed for CBH@TpAzo-foam_5 structure because the maximum interaction is taking place between the atoms of CBH and TpAzo foam. The E_{int} is -497.27 kJ $mol^{-1}$for CBH@TpAzo-foam_5, which illustrates the maximum stability due to the four H-bonds. However, the number of hydrogen bonds reduces to two in CBH@TpAzo-foam_4, thus the E_{int} also reduces to -171.45 kJ mol^{-1}. For the structures CBH@TpAzo-foam_1, CBH@TpAzo-foam_2, and CBH@TpAzo-foam_3, the interactions are taking place on the surface of top layer with the D_{int} >3.00 Å, especially for CBH@TpAzo-foam_1 and CBH@TpAzo-foam_3. The E_{int} are -36.97, -117.69, and -140.75 kJ mol^{-1} respectively for CBH@TpAzo-foam_1, CBH@TpAzo-foam_2, and CBH@TpAzo-foam_3. The interaction energies and interaction distances of CBH@TpAzo-foam_1 and CBH@TpAzo-foam_3 illustrate the weak dispersion forces dominate in stabilizing these structures.

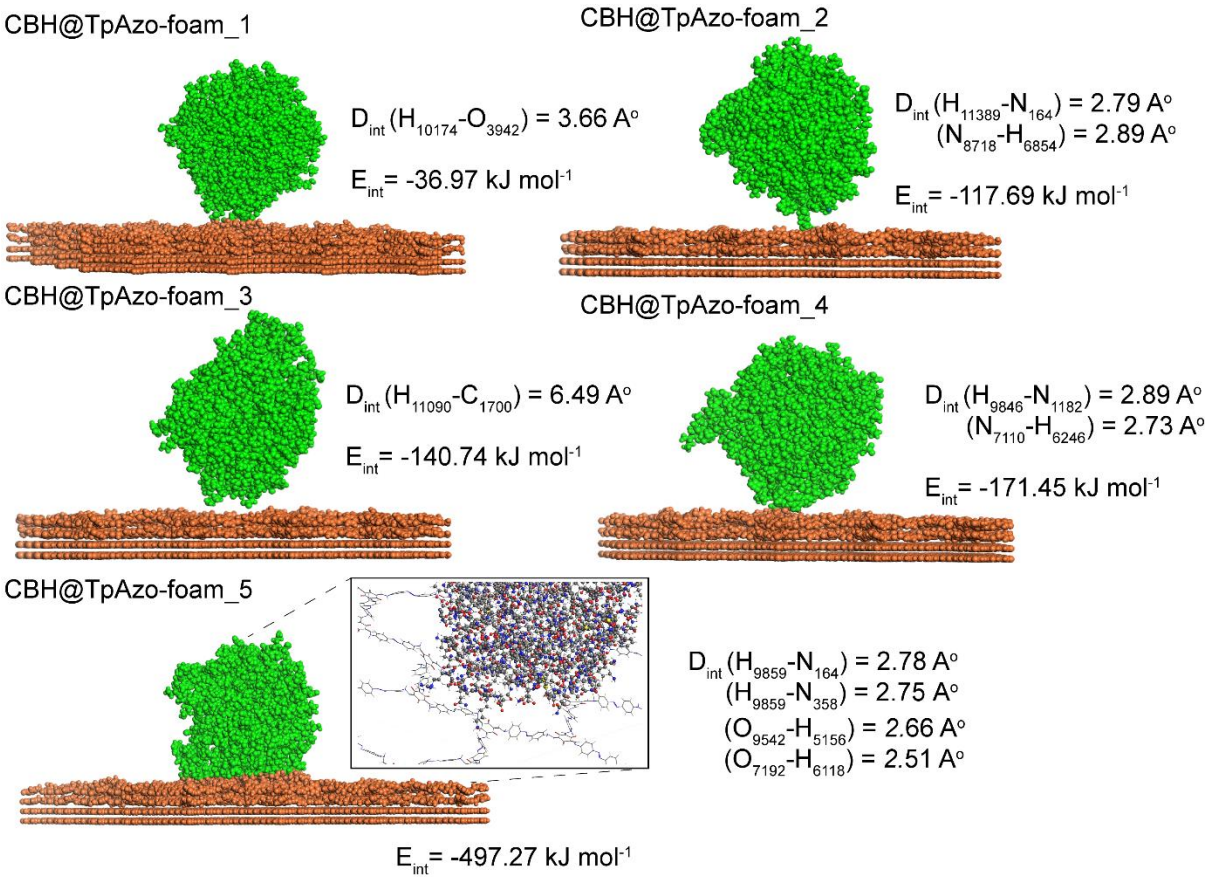

Figure S29. Five interaction geometries of CBH and TpAzo foam.

Unlike BGL and CBH, all the structures of EG are stabilized by H-bonding. Therefore, the interaction stability is highest for EG@TpAzo-foam structures. The $D_{int/s}$ between enzyme and TpAzo foam in EG@TpAzo-foam_1, EG@TpAzo-foam_2, EG@TpAzo-foam_3, EG@TpAzo-foam_4, and EG@TpAzo-foam_5 are 2.67, 2.72, 2.36, 2.55 and 2.31 Å; correspondingly, the $E_{int/s}$ are -270.90, -360.58, -419.80, -421.23 and -667.58 kJ mol^{-1}, respectively. Finally, it can be concluded that the EG interacts more strongly to TpAzo foam due to the greatest amount of observable H-bonding interactions, which is followed by the BGL while CBH shows the least interaction with the TpAzo foam layers.

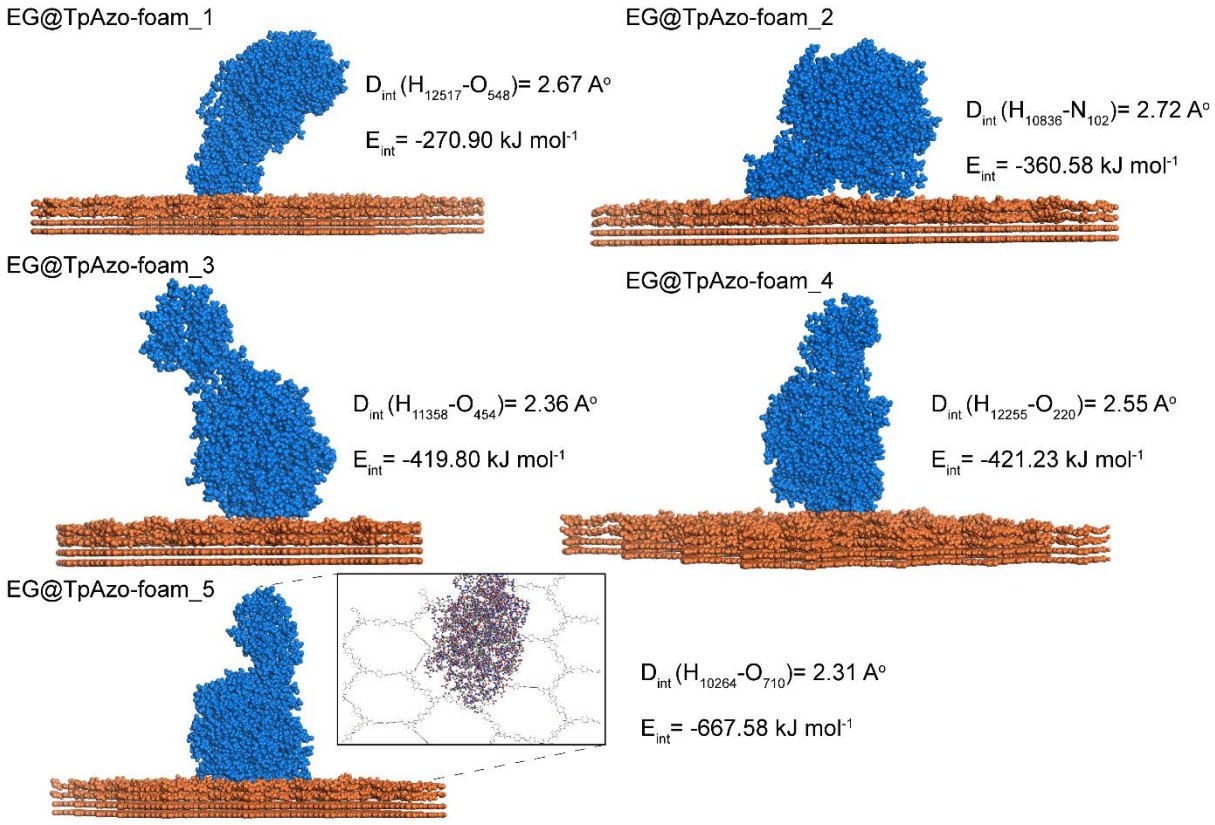

Figure S30. Five interaction geometries of EG and TpAzo foam.

Table S3. Key Enzyme-TpAzo foam interactions, distances (D_{int}), energies (E_{int}), and separation between enzymes of unit cells.

Enzyme-BGL				
Species	A_{int}	D_{int} (Å)	E_{int} (kJ mol^{-1})	D_{E---E} (Å)
BGL@TpAzo-foam_1	O_{10371}-H_{4838}	3.66	-93.51	76.60
BGL@TpAzo-foam_2	O_{7687}-H_{5990}	2.60	-131.62	84.87
BGL@TpAzo-foam_3	O_{7374}-H_{6758} H_{13867}-N_{414}	2.75 2.99	-164.58	82.61
BGL@TpAzo-foam_4	N_{9070}-H_{5052} O_{9061}- H_{5532} O_{9003}-H_{6110} O_{9069}-H_{6236} N_{9129}-H_{6300}	2.98 2.56 2.60 2.58 2.71	-349.53	83.08
BGL@TpAzo-foam_5	N_{124}-H_{13722} H_{12001}-N_{360} H_{13770}-N_{414} H_{13775}-N_{414} H_{12411}- O_{550} H_{12408}-O_{614} O_{9848}-H_{4710} O_{10376}-H_{5286}	2.93 2.90 2.94 2.72 2.96 2.91 2.90 2.77	-554.47	72.57

	O_{10371}-H_{5670} O_{7268}-H_{6342} O_{10376}-H_{6438} O_{7218}-H_{6493} O_{7268}- H_{6526} N_{7257}- H_{6558} O_{7260}- H_{6558} O_{10359}- H_{6822}	2.56 2.81 2.87 2.86 2.70 2.89 2.89 2.67		
Enzyme-CBH				
CBH@TpAzo-foam_1	H_{10174}-C_{3942}	3.66	-36.97	77.42
CBH@TpAzo-foam@_2	H_{11389}-N_{164} N_{8718}-H_{6854}	2.79 2.89	-117.69	73.55
CBH@TpAzo-foam_3	H_{9846}-N_{1182} N_{7110}-H_{6246}	6.49	-140.74	76.05
CBH@TpAzo-foam_4	H_{11090}-C_{1700}	2.89 2.73	-171.45	80.45
CBH@TpAzo-foam_5	H_{9859}-N_{164} H_{12166}-N_{164} H_{9859}-N_{358} H_{12018}-O_{612} H_{9871}-O_{806} H_{9874}-O_{806} O_{7169}-H_{4966} O_{9542}-H_{5156} O_{7192}-H_{6118} O_{8735}-H_{6494} O_{7192}-H_{6886}	2.78 2.83 2.75 2.95 2.88 2.79 2.91 2.66 2.51 2.81 2.89	-497.27	82.66
Enzyme-EG				
EG@TpAzo-foam_1	H_{12516}-O_{548} H_{12517}-O_{548} O_{9440}-H_{5220} O_{9446}-H_{5220} O_{9659}-H_{5476} O_{9446}-H_{5640} N_{9665}-H_{5860} O_{9683}-H_{5924}	2.82 2.67 2.78 2.82 2.89 2.70 2.73 2.80	-270.90	92.10
EG@TpAzo-foam_2	H_{10836}-N_{102} H_{10804}-O_{550} O_{7884}-H_{6054} O_{7830}-H_{6246}	2.85 2.72 2.88 2.85	-360.58	92.08
EG@TpAzo-foam_3	H_{11337}-N_{414} H_{11338}-N_{414} H_{11358}-O_{454} H_{11360}-O_{454} H_{11354}-O_{486} H_{11358}-O_{486}	2.85 2.75 2.36 2.77 2.48 2.80	-419.80	82.02

	H_{11076}-O_{550}	2.84		
	H_{11036}-O_{614}	2.77		
	O_{8403}-H_{4838}	2.76		
	O_{8216}-H_{4838}	2.65		
	O_{8184}-H_{5670}	2.65		
	O_{8205}-H_{5734}	3.00		
	N_{8417}-H_{5862}	2.66		
	N_{8400}-H_{5990}	2.81		
	O_{8391}-H_{6558}	2.96		
EG@TpAzo-foam_4	H_{12255}-N_{220}	2.75	-421.23	79.56
	H_{12255}-N_{220}	2.55		
	N_{8545}-H_{4710}	2.89		
	N_{9373}-H_{5596}	2.91		
	O_{9539}-H_{5662}	2.81		
	O_{9535}-H_{6430}	2.67		
	N_{9380}-H_{6652}	2.83		
EG@TpAzo-foam_5	H_{10877}-N_{156}	2.78	-667.58	82.90
	H_{10514}-N_{230}	2.96		
	H_{10485}-N_{414}	3.00		
	H_{10264}-O_{710}	2.31		
	H_{10845}-O_{734}	2.88		
	H_{11984}-O_{806}	2.80		
	H_{11987}-O_{806}	2.98		
	H_{11994}-O_{806}	2.83		
	H_{11993}-N_{1190}	2.97		
	O_{7347}-H_{5156}	2.78		
	O_{9120}-H_{5350}	2.97		
	O_{9123}-H_{5350}	2.38		
	O_{7239}-H_{6054}	2.78		
	O_{7283}-H_{6276}	2.95		
	O_{7282}-H_{6308}	2.88		
	O_{7282}-H_{6308}	2.71		
	O_{7265}-H_{6630}	2.49		
	O_{7283}-H_{6854}	2.94		

Section S-16

References

[1] J. H. Chong, M. Sauer, B. O. Patrick, M. MacLachlan, J. Org. Lett. 2003, **5**, 3823-3826.

[2] A. Halder, S. Kandambeth, B. P. Biswal, G. Kaur, N. C. Roy, M. Addicoat, J. K. Salunke, S. Banerjee, K. Vanka, T. Heine, S. Verma, R. Banerjee, *Angew. Chemie - Int. Ed.* 2016, **55**, 7806–7810.

[3] S. Goswami, N. Gupta, S. Datta, *Biotechnol. Biofuels* 2016, **72**, 9.

[4] E. Gasteiger, A. Bairoch, J. C. Sanchez, K. L. Williams, R. D. Appel, D. F. Hochstrasser, M. R. Wilkins, *Methods Mol. Biol.* 1999, **112**, 531–52.

[5] J. Ohser, F. Mücklich. Statistical Analysis of Microstructures in Materials Science, 2001

[6] G. Velde, E. J. Baerends, F. M. Bickelhaupt, E. J. Baerends, C. Fonseca Guerra, S. J. a. van Gisbergen, J. G. Snijders, T. Ziegler, G. T. E. Velde, C. F. Guerra, S. J. a V. a N. Gisbergen, *J. Comput. Chem.* 2001, **22**, 931–967.

[7] S. Grimme, C. Bannwarth, P. Shushkov, *J. Chem. Theory Comput.* 2017, **13**, 1989–2009.

[8] M. Nurhuda, C. C. Perry, M. A. Addicoat, *Phys. Chem. Chem. Phys.* 2022**.**

[9] K. S. Colwell, C. J. Casewit, W. A. Goddard, W. M. Skiff, A. K. Rappe, C. J. Casewit, K. S. Colwell, W. A. Goddard III, W. M. Skiff, *J. Am. Chem. Soc.* 2005, **114**, 10024–10035.

[10] S. Nosé, *Mol. Phys.* 1986, **57**, 187–191.

[11] M. Svensson, S. Humbel, R. D. J. Froese, T. Matsubara, S. Sieber, K. Morokuma, *J. Phys. Chem.* 1996, **100**, 19357–19363.

[12] T. F. Willems, C. H. Rycroft, M. Kazi, J. C. Meza, M. Haranczyk, *Microporous Mesoporous Mater.* 2012, **149**, 134–141.